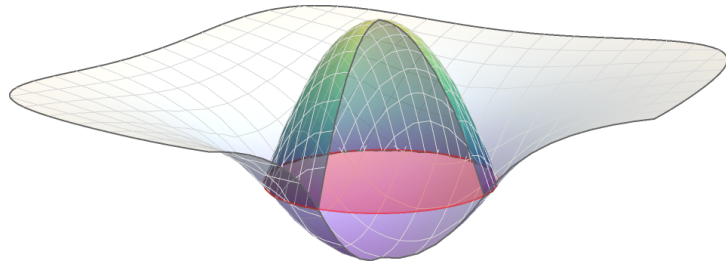


# Ultraviolet regular Black Holes

## Master Thesis

SVEN KÖPPEL

October 2014



*First Supervisor:* PD DR. PIERO NICOLINI

*Second Supervisor:* PROF. DR. MARCUS BLEICHER

INSTITUTE FOR THEORETICAL PHYSICS &  
FRANKFURT INSTITUTE FOR ADVANCED STUDIES



Vorliegende Version ist vom **October 19, 2014, 21:07**

## Abstract

In this thesis, I present a family of Black Hole geometries exposing a modified minimal length scale behaviour due to the gravity self-complete paradigm. I extend these geometries to the ADD large extra-dimensional scenario. This allows Black Hole remnant masses to reach the TeV scale. We show that the evaporation endpoint for this class of Black Holes is a cold stable remnant. While the one geometry features a regular deSitter core that counters gravitational collapse with a quantum outward pressure, the other geometry turns out to fit nicely into the holographic information bound on Black Holes, leading to Black Hole area quantization and applications in the Black Hole entropic force, deriving gravity as emergence phenomena from the fundamental thermodynamics.

The thesis contains an overview about recent quantum gravity Black Hole approaches and concludes with the derivation of nonlocal operators that modify the Einstein equations to ultra-violet safe field equations.

## Master thesis

*written at*

### **Institut für theoretische Physik**

Fachbereich Physik  
Goethe-Universität Frankfurt am Main  
Max-von-Laue-Straße 1  
60438 Frankfurt am Main

*and*

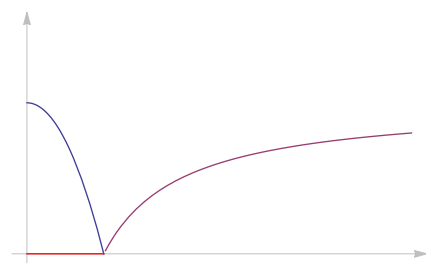
### **Frankfurt Institute for Advanced Studies (FIAS)**

Ruth-Moufang-Straße 1  
60438 Frankfurt am Main

## About the front picture

This picture visualizes a kind of Black Hole proposed in this thesis, compared with the classical Schwarzschild Black Hole (the well known “cone”). The red disk indicates the position of the event horizon: Anything “inside” the disk cannot get out of it.

More strictly, the 3-dimensional illustration shows an embedding of the equatorial plane of the equatorial plane of the self-regular Black Hole which gravitational potential is e.g. shown in figure 3.4 for  $\alpha \rightarrow \infty$ . For the sake of better understanding, there is a cut-out to view the inside of the object. The picture can be constructed by rotating the graph shown on the right around its  $y$  axis.



# Contents

Introduction . . . . .	5
Outline . . . . .	6
<b>1 Gravitation</b>	<b>7</b>
1.1 General Relativity . . . . .	7
1.1.1 Differential Geometry . . . . .	7
1.1.2 Covariant Derivation Operator . . . . .	7
1.1.3 The Metric . . . . .	8
1.1.4 Curvature . . . . .	8
1.1.5 Einstein Field Equations . . . . .	9
1.2 Exact solutions of General Relativity . . . . .	10
1.2.1 Minkowski space-time . . . . .	10
1.2.2 Schwarzschild metric . . . . .	11
1.2.3 De Sitter space-time . . . . .	11
1.3 Higher dimensional Gravity . . . . .	12
1.3.1 Kaluza Klein theory . . . . .	13
1.3.2 Randall-Sundrum scenario . . . . .	13
1.3.3 ADD-model and Large Extra Dimensions . . . . .	13
1.3.4 Black Holes in particle detectors . . . . .	15
<b>2 Short-scale improved Black Holes</b>	<b>16</b>
2.1 Black hole evaporation phases . . . . .	16
2.2 Problems of the Schwarzschild Black Hole . . . . .	17
2.3 Quantum Gravity Black Holes . . . . .	18
2.4 Requirements for self-complete Black Hole metrics . . . . .	21
2.5 Quasi-classical source terms . . . . .	21
2.5.1 Derivation of the metric . . . . .	21
2.5.2 Smeared matter density . . . . .	23
2.6 Choices for mass profiles and their $d$ -dimensional extension . . . . .	23
2.6.1 Extension to extra dimensions . . . . .	24
2.6.2 Length scales . . . . .	24
2.6.3 The Schwarzschild limit . . . . .	24
<b>3 Geometry of the Black Holes</b>	<b>25</b>
3.1 The Mass . . . . .	25
3.2 Horizons . . . . .	25
3.3 The self-encoding remnant . . . . .	27
3.4 The regular core . . . . .	29
3.5 Conformal Structure . . . . .	31
3.6 Energy conditions . . . . .	33

<b>4 Thermodynamical properties</b>	<b>34</b>
4.1 Hawking Temperature . . . . .	34
4.2 Heat capacity . . . . .	36
4.3 The Phase transition . . . . .	38
4.4 Entropy . . . . .	40
4.4.1 The area quantization picture . . . . .	40
<b>5 Modified field equations</b>	<b>42</b>
5.1 Higher-dimensional Fourier Transformation . . . . .	43
5.2 Deriving the bilocal smearing operator . . . . .	44
5.2.1 Holographic modified Einstein equations . . . . .	44
5.2.2 Self-encoding modified Einstein equations . . . . .	46
<b>6 Conclusion</b>	<b>47</b>
<b>Appendix</b>	<b>48</b>
<b>A All forms of <math>H</math></b>	<b>48</b>
<b>B <math>n</math>-spheres</b>	<b>49</b>
<b>C Details of the radial symmetric <math>d</math>-dimensional FT</b>	<b>50</b>
C.1 Review of the 3d Fourier transformation . . . . .	50
C.2 Analytic continuation of the Heaviside step function . . . . .	51
<b>D Detailed Tensors in the spherical symmetry calculation and a formulary</b>	<b>51</b>
D.1 Christoffel symbols . . . . .	52
<b>List of figures and tables</b>	<b>53</b>
<b>Bibliography</b>	<b>54</b>
<b>Acknowledgement</b>	<b>59</b>
<b>Declaration of independence</b>	<b>59</b>

# Introduction

This work is about the quest of contemporary physics on the smallest scales and with the biggest energies. By historical evolution, in the 20th century two opposing theories developed: Quantum Physics, which is the physics at smallest scales and produced confusing paradoxa like Schrödinger's cat, and on the other hand relativistic physics, which is physics at the biggest scales and lead to General Relativity, the theory for space and time presented by Albert Einstein in 1915.

The combination of Quantum Mechanics and Special Relativity lead to Quantum Field Theory (QFT) and the formulation of the Standard Model of particle physics which is exceptionally and unexpectedly successful. From the viewpoint of an high-energy physicist, three of four fundamental interactions, namely the electromagnetic, weak nuclear and strong nuclear interactions have been successfully joined in a unified theory, and gravity is simply the weakest and last interaction left as an "ordinary" field theory. On the other hand, from the viewpoint of a relativist, General Relativity taught us that there is no background space where physics "happens". This new principle lead to a bunch of new physics, where the most remarkable is perhaps the existence of Black Holes as trapped areas in spacetime or even the existence of wormholes (Einstein-Rosen bridge). Certainly, General Relativity had the bigger impact on the science fiction genre.

Physics beyond the Standard Model is an uncomfortable job. On the one hand, such physics lack experimental accessibility. Theoretically, the best thing we can do starting from QFT is curved space quantum field theory, that is, calculating quantum fields on a curved space background, but without space-matter interaction. In the *cube of physical theories*, as shown in figure 0.1, this is probably the half way to the "Theory of Everything".

Actually, curved space QFT opened the door for the first quantum mechanical treatments of strong gravitational objects: Black Holes. In the 1970s, this lead to Hawking's groundbreaking prediction of thermal radiation of Schwarzschild Black Holes. In terms of "theories", Hawking radiation is really interdisciplinary:

$$T_H = \frac{\hbar c^3}{8\pi G M k_B}$$

There are "ingredients" from Quantum Mechanics (Planck constant  $\hbar$ ), Special Relativity (speed of light  $c$ ), Gravitation (Newton's constant  $G$ ) and Thermodynamics (Boltzmann constant  $k_B$ ).

But Hawking's temperature also contains the failure of General Relativity: The temperature increases with decreasing mass  $M$ , since it is written in the denominator. Since radiating Black Holes loose mass, they get hotter and hotter. If there are Black Holes (and there is a strong sense there are), the universe should be hot, but it is not.

In this thesis, I propose modifications to General Relativity dealing with this kind of *big mass* problem. As in physics, big mass correspond with high energy and low distance, we use the term *ultra-violet*, coming from the wavy nature of light, to describe an high energy regime. This thesis deals with ultra-violet corrections of the most simple Black Hole possible, the Schwarzschild Black Hole.

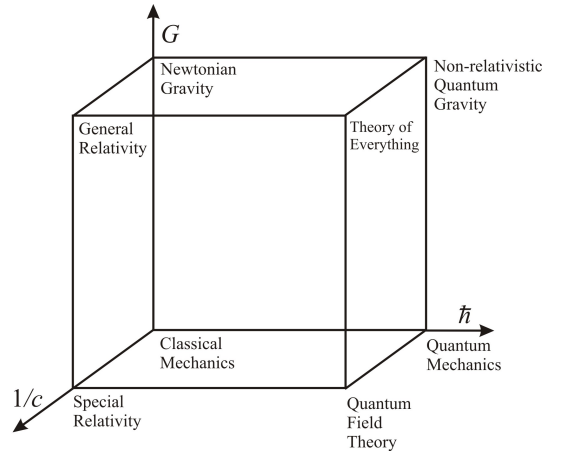


Figure 0.1: The *cube of physics*, a popular illustration about characteristic constants that describe the regime for physical phenomena. First appeared in a 1999 book from Penrose [60].

## Outline

Section 1 is an introductory section about General Relativity. It will give an introduction to the formalism and shortly derive the Einstein equation. Then the first solutions on GR are shown and the different types of singularities and their origins are discussed. An outline about gravity in extra dimensions and the issue of observations of micro Black Holes is given.

Section 2 is devoted to the shortest scales of Black Holes. It deals with the breakdown of the Schwarzschild description in the Planck phase of Black Hole evaporation and presents various Quantum Gravity approaches to describe the Planck phase. In contrast, afterwards a short scale modification will be introduced that does not relies on a theory *beyond* General Relativity. To do so, Einstein Equations are solved for an ideal static isotropic “blurred” matter ball that shall describe a “quasi-classical” mass point. Two such profiles are presented under the name *holographic* and the *self-regular* mass profile. They are extended to the large extradimensional scenario.

In section 3, the geometry of the mass profiles is derived and discussed. The analogy to the Reissner-Nördstrom space-time becomes apparent. The appearance of a Black Hole *remnant* as smallest *self-encoding* building block of matter is described, it motivates to call General Relativity *self-complete* on minimal length scales. The regular DeSitter core of a Black Hole with its quantum interpretation is discussed.

Section 4 approaches the thermodynamical properties of this class of Black Holes. The associated temperature, heat capacity and entropy are derived and a phase transition at some critical radius is found. Concerning the entropy, the meaning of *holography* in gravity and possible outcomes for the Black Hole information paradox are explained.

In section 5, the Einstein field equations are modified in order to find a dual nonlocal gravity theory that gives the same results as the purely-Einsteinian matter. Such a theory may be called a *quantum improved* General Relativity, as it incorporates short scale improvements in the context of tensor calculus and Riemannian geometry.

# Chapter 1

## Gravitation

### 1.1 General Relativity

In this section, a short derivation of General Relativity (GR) is given. It is the geometrical theory of gravitational interaction from matter and the major framework used in this work. To do so, some core concepts of differential geometry on manifolds are retraced briefly in order to derive the Einstein Field Equations (EFE) by Hamiltonian's principle of least action. Exact definitions of the new vector concept are skipped in favour of condensing the ideas. In this text I follow the notations of [13, 42, 46, 75, 76]. They prefer “index free” notation as a more fundamental approach to introduce Riemannian geometry. In contrast, some tensors may also be derived by “index constraints” as done in [26]. This is less elegant but more straightforward.

#### 1.1.1 Differential Geometry

In curved space geometry, intuition about well-known mathematical symbols like vectors as “position vectors” fails [76]. The mathematical approach is a differential description using the fact that manifolds  $M$  look “nearly” flat. Thus the tangent vector  $V$  is introduced as a directional derivative operator. The components of such a vector may be denoted as

$$V^\mu(f) = V^\mu \frac{\partial f}{\partial x^\mu}. \quad (1.1)$$

The vector  $V$  maps functions  $f \in C^\infty(M, \mathbb{R})$  to  $\mathbb{R}$ . With a fixed point  $p \in M$ , it defines the tangent vector space  $V_p$ . Introducing the dual space  $V_p^*$  and the dual dual space  $V_p^{**} \cong V_p$  yields to the definition of tensors as a multilinear mappings from vectors and dual vectors into numbers [75].

#### 1.1.2 Covariant Derivation Operator

As for two points  $p, q \in M$ , the tangent spaces  $V_p$  and  $V_q$  can not directly be compared: Defining for the vector  $V^\mu$  a traditional derivative (cf. [46, page 208])

$$\frac{\partial V^\mu}{\partial x^\nu} = \lim_{h \rightarrow 0} \frac{V^\mu(x^1, \dots, x^\nu + h^\nu, \dots, x^n) - V^\mu(x^1, \dots, x^\nu, \dots, x^n)}{h^\nu} \quad (1.2)$$

fails as even  $x$  and  $x + h$  may not be compared directly. As a solution, a covariant derivation operator  $\nabla$  by means of the parallel transport is derived. This operator will transform like a tensor.

While Wald [75, page 31] designates requirements for the covariant derivation (linearity, Leibnitz rule, index contraction commutativity, consistency with the index free notation and vanishing torsion tensor/commutativity) and derives the existence of a *connection coefficient*  $\Gamma_{bc}^a$ , one can also introduce the connection coefficient as the link in the parallel transport which shall be the “correct” way to denote the derivative (1.2):

$$V^\mu(x \rightarrow x + h) := V^\mu(x) - V^\lambda(x)\Gamma_{\nu\lambda}^\mu h^\nu. \quad (1.3)$$

By replacing the traditional difference  $V^\mu(x) - V^\mu(x + h)$  by  $V^\mu(x) - V^\mu(x \rightarrow x + h)$  in equation (1.2), one immediately ends up with the definition of the covariant derivative

$$\nabla_\mu V^\nu = \partial_\mu V^\nu + \Gamma_{\mu\sigma}^\nu V^\sigma. \quad (1.4)$$

The covariant derivative naturally extends when computing derivatives of tensors of arbitrary rank. For a  $(k, l)$ -Tensor  $T$  the derivative is given (without proof) by

$$\nabla_\alpha T_{\mu_1 \dots \mu_l}^{\lambda_1 \dots \lambda_k} = \partial_\alpha T_{\mu_1 \dots \mu_l}^{\lambda_1 \dots \lambda_k} + \sum_{i=1}^k \Gamma_{\alpha\beta}^{\lambda_i} T_{\mu_1 \dots \mu_l}^{\lambda_1 \dots \beta \dots \lambda_k} - \sum_{j=1}^l \Gamma_{\alpha\mu_i}^\beta T_{\mu_1 \dots \beta \dots \mu_l}^{\lambda_1 \dots \lambda_k}. \quad (1.5)$$

### 1.1.3 The Metric

The connection symbol  $\Gamma_{\beta\gamma}^\alpha$  introduced in equation (1.3) is still ambiguous. As soon as one equips the manifold with a metric  $g_{\mu\nu}$ , there is a special choice, constrained by the requirement that scalars shall be invariant under parallel transport (in colloquial terms, scalars are required to be the same in any coordinate system). The inner product of two arbitrary vectors  $v^\beta$  and  $w^\gamma$  is a scalar and shall therefore also be invariant under any parallel transport  $t^\alpha \nabla_\alpha$ . This leads to

$$0 \stackrel{!}{=} t^\alpha \nabla_\alpha g_{\beta\gamma} v^\beta w^\gamma \Rightarrow 0 = \nabla_\alpha g_{\beta\gamma}. \quad (1.6)$$

A connection  $\Gamma_{\alpha\beta}^\gamma$  is called *metric compatible* if it fulfills (1.6) and is torsion-free ( $\Gamma_{\alpha\beta}^\gamma = \Gamma_{(\alpha\beta)}^\gamma$ ), see e.g. [13, page 99] for torsion.

This uniquely determined choice of connection symbols is called *Christoffel symbols*. They allow computing the parallel transport and the covariant derivative from the metric:

$$\Gamma_{\alpha\beta}^\delta = \frac{1}{2} g^{\delta\gamma} (\partial_\alpha g_{\beta\delta} + \partial_\beta g_{\alpha\delta} + \partial_\gamma g_{\alpha\beta}). \quad (1.7)$$

### 1.1.4 Curvature

It is important to remember that for a manifold  $M$  there exist different choices of coordinate systems, and only if one found flat space coordinates that are applicable everywhere (that is,  $\Gamma = 0$  for all  $p \in M$ ), the manifold is not curved. This reasoning does not work the other way, as the example of choosing polar coordinates  $(t, r, \phi, \theta)$  in flat space shows: Some entries are non-zero (e.g.  $\Gamma_{r\phi}^\phi = 1/r$ ), but the space is still flat.

In favour to get a measure for spacetime curvature, one can analyse the “defects” of parallel transport around a closed loop with infinitesimal extend. It will be shown that the change is described by a  $(1, 3)$ -curvature tensor called *Riemann curvature tensor*.

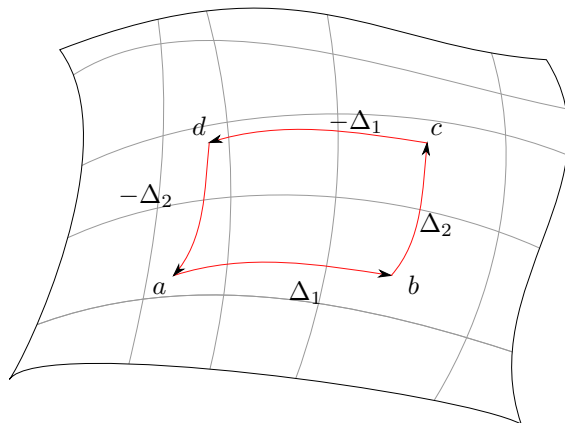


Figure 1.1: Illustration of the closed loop parallel transport on infinitesimal linear displacements  $\Delta_i^\mu$ . When performing the calculation in equation 1.8, on curved spacetimes one finds a defect which defines the Riemann tensor. This means the vector at the beginning (point a) does not match the vector after the loop any more.

In the present setup (cf. figure 1.1), the vector  $V^\mu$  is moved around the closed path  $a \rightarrow b \rightarrow c \rightarrow d$  with infinitesimal spacings  $+\Delta_1^\mu, +\Delta_2^\mu, -\Delta_1^\mu, -\Delta_2^\mu$ . One can determine the missing part  $\#$  when coming back to  $a$  by explicit computation of the vector  $V^\mu$  at the space time points:

$$V^\mu(a) = V^\mu(a) \quad (1.8a)$$

$$V^\mu(b) = V^\mu(a \rightarrow a + \Delta_1) = V^\mu(a) - V^\alpha(a)\Gamma_{\beta\alpha}^\mu(a)\Delta_1^\beta \quad (1.8b)$$

$$V^\mu(c) = V^\mu(b \rightarrow b + \Delta_2) = V^\mu(b) - V^\gamma(b)\Gamma_{\delta\gamma}^\mu(b)\Delta_2^\delta \quad (1.8c)$$

$$V^\mu(d) = V^\mu(c \rightarrow c - \Delta_1) = V^\mu(c) - V^\epsilon(c)\Gamma_{\kappa\epsilon}^\mu(c)(-\Delta_1^\kappa) \quad (1.8d)$$

$$\#V^\mu(a) = V^\mu(d \rightarrow d - \Delta_2) = V^\mu(d) - V^\lambda(d)\Gamma_{\omega\lambda}^\mu(d)(-\Delta_2^\omega) \quad (1.8e)$$

Recursively inserting all equations into each other gives a long expression where all linear terms  $\mathcal{O}(\Delta_i^\nu)$  vanish. All third powers  $\mathcal{O}(\Delta_i^\nu \Delta_j^\xi \Delta_k^\rho)$  are ignored, so the result is proportional to second order terms  $\mathcal{O}(\Delta_1^\gamma \Delta_2^\delta)$  after appropriate index relabeling. Note that the Christoffel symbols (also) depend on the point where they are evaluated at. They can be simply moved e.g. at the first insertion step 1.8b into 1.8c by  $\Gamma(b) = \Gamma(a) + \partial_\nu \Delta_1^\nu \Gamma(a)$ . One ends up with the definition of the Riemann tensor  $R_{\alpha\beta\gamma}^\mu$  as piece of the missing part

$$\#V^\mu(a) = V^\mu(a) \underbrace{\left( \partial_\beta \Gamma_{\gamma\alpha}^\mu - \partial_\gamma \Gamma_{\beta\alpha}^\mu + \Gamma_{\gamma\alpha}^\delta \Gamma_{\beta\delta}^\mu - \Gamma_{\beta\alpha}^\delta \Gamma_{\gamma\delta}^\mu \right)}_{R_{\alpha\beta\gamma}^\mu} \Delta_1^\gamma \Delta_2^\delta. \quad (1.9)$$

By tensor contraction, one can define the simpler Ricci tensor  $R_{\mu\nu} = R_{\mu\lambda\nu}^\lambda$  and finally the Ricci scalar  $R = R_\lambda^\lambda$ . This quantity is also called scalar curvature and it is the simplest invariant that gives information about flatness of space: As soon as  $R = 0$  everywhere, the space is flat.

Most significance for the next section has the Einstein curvature tensor

$$G_{\mu\nu} = R_{\mu\nu} + \frac{1}{2}g_{\mu\nu}R. \quad (1.10)$$

### 1.1.5 Einstein Field Equations

Einstein equations can be derived from a variational principle  $\delta S = 0$  on the action  $S$  (Hamilton principle). They can also be derived by other means, e.g. symmetry aspects leaving only one choice for combining  $G_{\mu\nu}$  and the energy density tensor  $T_{\mu\nu}$ .

Here, the ansatz will be the action, defined by the Lagrangian  $\mathcal{L} = \mathcal{L}_G + \mathcal{L}_M$ , that is, the interaction (gravitational) part and the source (matter) part. Those two parts are guessed, and basically taking the curvature scalar  $R$  and the trace of the energy density tensor  $T = T_\lambda^\lambda$  appears to be both an intuitive and good choice. The low energy matching is traditionally accomplished by a prefactor  $\kappa$ , so one ends up with the *Einstein-Hilbert-Action* including matter,

$$S = \int \sqrt{-g} \, d^4x \left( \frac{R}{2\kappa} + T \right) \quad (1.11)$$

Note that  $\sqrt{-g}$ , with  $g$  the determinant of the metric  $g^{\mu\nu}$ , is necessary for the invariant volume element.

Splitting up the integral into two parts  $S_R$  and  $S_T$  and calculate the variation individually yields, at first for  $S_R$ ,

$$\delta S_R = \frac{1}{2\kappa} \delta \int \sqrt{-g} \, d^4x \, R_{\mu\nu} g^{\mu\nu} = \frac{1}{2\kappa} \int d^4x \, R_{\mu\nu} \delta(\sqrt{-g} g^{\mu\nu}) + \frac{1}{2\kappa} \int d^4x \, \sqrt{-g} g^{\mu\nu} (\delta R_{\mu\nu}). \quad (1.12)$$

One can show that the integral over the variation of  $\delta R_{\mu\nu}$  vanishes (surface integral) while the variation  $\delta \sqrt{-g} g^{\mu\nu}$  contributes.

For a full discussion, one typically switches to *tensor densities* which are “salted” with  $\sqrt{-g}$  and written in German gothic letters [46]

$$\mathfrak{T}^{\dots} = \sqrt{-g} A^{\dots}, \quad (1.13)$$

where  $A_{\mu\nu}$  represents a tensor in a local coordinate frame. Using the identity  $\delta\sqrt{-g} = -1/2\sqrt{-g}g_{\mu\nu}\delta g^{\mu\nu}$  yields

$$\delta S_R = \int d^4x R_{\mu\nu}(\delta\sqrt{-g}g^{\mu\nu}) = \int d^4x \sqrt{-g} \left( R_{\mu\nu} - \frac{1}{2}g_{\mu\nu}R \right) \delta g^{\mu\nu}. \quad (1.14)$$

Secondly, considering  $S_T$ , it is

$$\delta S_T = \int d^4x \sqrt{-g} (\kappa T_{\mu\nu}) \delta g^{\mu\nu}. \quad (1.15)$$

By requiring  $\delta_S = \delta S_R + \delta S_T = 0$  and collecting the terms under the integrals one receives

$$R_{\mu\nu} - \frac{1}{2}g_{\mu\nu}R = \kappa T_{\mu\nu}, \quad (1.16)$$

the *Einstein Field Equations* (EFE). The low energy matching with the Newtonian potential  $\Phi = -GM/r$  allows determining  $\kappa = -8\pi G$  (with  $G$  the Newton constant, not to be confused with the rarely used trace of the Einstein tensor  $G^\mu_\mu$ ).

An astonishing fact of the Einstein field equations is that they allow deriving all classical predictions of mechanics. The energy conservation law  $\nabla_\mu T^{\mu\nu} = 0$  is also intrinsically contained in the Einstein field equations. One can show that in  $d = 3+1$  space-time dimensions, the EFE are 10 independent non-linear coupled equations which are only possible to solve analytically for highly symmetric problems.

## 1.2 Exact solutions of General Relativity

There are books collecting and classifying exact solutions (in contrast to numerical solutions or expansions) of Einstein gravity like Griffiths [31] and Stephani [68]. For an introductory overview about the spacetimes developed by Schwarzschild and DeSitter which are presented in this section, Griffiths text book [31] gives the best overview, this section follows the reasoning of Griffiths.

In this section, in favour to the derivation of a quasi-classical source term in section 2.5, the metrics are not derived.

### 1.2.1 Minkowski space-time

This section is for fixing the notation used in the thesis. Minkowski spacetime (the flat space) is the Einstein solution of the empty space  $R_{\mu\nu} = 0$ . Working in cartesian coordinates and considering flat space with a  $g_{\mu\nu} = \eta_{\mu\nu} = \text{diag}(-1, +1, +1, +1)$  signature, the Minkowski line element can be given as

$$ds^2 = g_{\mu\nu}dx^\mu dx^\nu = -dt^2 + dx^2 + dy^2 + dz^2, \quad (1.17)$$

with the coordinates  $t, x, y, z \in (-\infty, \infty)$ . It is convenient to switch to spherical coordinates when a spherical symmetric problem is given (as it is, in this thesis). Spherical coordinates can be given by the transformation rules  $x = r \sin \theta$ ,  $y = r \sin \theta \sin \phi$  and  $z = r \cos \theta$ , with  $r \in [0, \infty)$ ,  $\theta \in [0, \pi]$  and  $\phi \in [0, 2\pi]$ . In these coordinates, the (same) line element reads

$$ds^2 = -dt^2 + dr^2 + r^2(d\theta^2 + \sin^2 \theta d\phi^2) = -dt^2 + dr^2 + r^2 d\Omega_2^2. \quad (1.18)$$

Considering spherical coordinates in flat Minkowski space is a good opportunity to learn about *coordinate singularities*: Apparently, the spherical line element (1.18) exhibits singularities at points where  $r = 0$ ,  $\sin \theta = 0$  or  $r \rightarrow \infty$ . But the cartesian coordinate choice (1.17) tells that these singularities are not “real”, because equation (1.17) shows coordinates without singularities, so the apparent singularities are no true singularities. In contrast, a *curvature singularity* is distinguished by a diverging curvature scalar  $R = R^\mu_\mu$ , and no choice of coordinates can avoid a coordinate singularity at points where a curvature singularity occurs. In the next section, the most simple space-time exposing a single curvature singularity point is encountered.

### 1.2.2 Schwarzschild metric

The Schwarzschild metric is the solution for the spherically symmetric static point mass distribution

$$\rho_\theta(r) := \frac{M}{4\pi r^2} \delta(r), \quad (1.19)$$

which is – having electrostatics in mind – the most basic distribution one can imagine.

The Schwarzschild problem, as can be found in text books [46, 75], is typically divided into the *outer* Schwarzschild metric, which describes the space outside a spherically symmetric static mass distribution where  $R_{\mu\nu} = 0$ , and the *interior* Schwarzschild metric that describes the space-time inside a perfect fluid.

It is worth mentioning that the outer Schwarzschild metric is derived from  $\rho_\theta(r)$ , as given in (1.19), but it will be assumed to be the solution for any  $\rho(r)$ . This is a consequence of the *Birkhoff theorem* which states that any spherically symmetric solution of the vacuum Einstein field equations must be static and *asymptotically* flat (Minkowski for  $r \rightarrow \infty$ ). Note that the Birkhoff theorem only holds in  $d = 4$  space-time dimensions (cf. the next section about higher dimensional gravity).

The solution of (1.19) is given by the Schwarzschild metric

$$dr^2 = (1 - 2\Phi(r))dt^2 - (1 - 2\Phi(r))^{-1}dr^2 - r^2d\theta^2 - r^2\sin^2(\theta)d\phi^2 \quad (1.20)$$

with the gravitational potential (Newton's potential)  $\Phi(r) = GM/r$ . Note that  $r$  is not the *distance* of the origin  $r = 0$ , as space time is deformed and  $r$  actually gets timelike for  $r < 2GM$ .

The radius  $r_0 = 2GM$  has a special meaning. At  $r_0$ , the metric (1.20) has a *coordinate* singularity which is not a curvature singularity, as one can see when switching e.g. to Eddington-Finkelstein coordinates (Tortoise coordinates). What physically happens at  $r_0$  is that light from the space time region enclosed by the  $r = r_0$  cannot escape that surface, it is literally trapped (*trapping* surface or trapped surfaces). For this reason, one calls this a *Black Hole* with event horizon radius  $r_0$ , as no event that takes place inside the horizon can be seen by an outside observer.

Actually, the Schwarzschild space-time features a curvature singularity at  $r = 0$ , which was already “announced” by the Dirac delta function,  $\rho_\theta(r) \xrightarrow{r \rightarrow 0} \infty$ . The singularity is shielded by the event horizon, so whatever happens near it cannot be observed outside. In 1969, Roger Penrose formulated the *cosmic censorship hypothesis* which states that curvature singularities are always “hidden” behind an event horizon, so there are no *naked singularities*. In fact, there are solutions of the EFEs with naked singularities, like the hyper-extreme Reissner-Nordström space-time, discussed in section 3.5.

Many modifications of the Schwarzschild line element have been investigated, e.g.  $g_{00} = 1 - 2GM/r \rightarrow \epsilon - 2GM/r$ , or by allowing  $M \rightarrow M(x)$ , or by including new physics (like electrical charge). Such approaches have been studied [31], and actually  $M \rightarrow M(r)$  in a way  $\delta \rightarrow h(r)$  with  $h(r)$  a finite delta approximation describes best the roadmap for this thesis. However, in any General Relativity text book, the Schwarzschild metric is almost always extended with angular momentum  $J$  and/or electric charge  $Q$ , as there exist the old and well-known solutions of the Reissner-Nordström (RN) metric ( $Q > 0, J = 0$ ), the Kerr metric ( $Q = 0, J > 0$ ) and the Kerr-Newman metric ( $Q, J > 0$ ). The *no-hair theorem*, formulated by John Wheeler, postulates that all Black Hole solutions resulting from the Einstein equations (including electromagnetism, so strictly spoken Einstein-Maxwell equations) are fully characterized by only mass  $M$ , electrical charge  $Q$  and angular momentum  $J$ . Actually, this theorem has not been proven and is therefore only a *conjecture* that will be addressed in section 2.1 again.

While angular momentum is probably the most relevant one for astronomical purpose, for this thesis it turns out that the RN metric possesses analogons to the regular Black Hole solutions that will be derived (section 3.5). Note that in this thesis, spinning Black Holes are not treated. This is not necessarily bad, since only the final evaporation phases of Black Holes is concerned. Section 2.1 will deal with that topic.

### 1.2.3 De Sitter space-time

Except the flat Minkowski space time, there are also two (unique) solutions with constant curvature  $R$ , which can be derived by the 10 isometries of space-time in four dimensional space-time by the local condition [31]

$$R_{\alpha\beta\gamma\delta} = \frac{R}{12}(g_{\alpha\gamma}g_{\beta\delta} - g_{\alpha\delta}g_{\beta\gamma}). \quad (1.21)$$

Using the Einstein equations with cosmological constant  $\Lambda$ ,

$$G_{\mu\nu} + \Lambda g_{\mu\nu} = 8\pi G T_{\mu\nu}, \quad (1.22)$$

these two solutions are real vacuum solutions ( $T_{\mu\nu} = 0$ ), and  $R = 4\Lambda$ ,  $R_{\alpha\beta} = \Lambda g_{\alpha\beta}$ . Space with  $R > 0$  is called *de Sitter* space-time (dS) while space with  $R < 0$  is called *anti-de Sitter* space-time (AdS), after the dutch physicist Willem de Sitter.

There is a set of spherical coordinates that does not cover the complete deSitter space time, but is well enough for the considerations done in this thesis. Robert Mayers calls these the “static patch” coordinates [50], and the gravitational potential is given by

$$V(r) = \frac{\Lambda}{3}r^2 := \left(\frac{r}{\ell}\right)^2. \quad (1.23)$$

In de Sitter space, our coordinates  $g_{00} = 1 - r^2/\ell^2$  expose a singularity at  $r_0 = \ell = \sqrt{3/\Lambda}$ . Of course, since  $R = 4\Lambda > 0$  everywhere, there is no curvature singularity, but the surface  $r = \ell$  forms a horizon. One can derive that this is a *cosmological horizon* [31] which reveals that the universe expansion speed is higher than the speed of light and events beyond  $r > \ell$  cannot reach the observer at  $r = 0$  anymore. An exact discussion requires introduction of Friedmann-Lemaître-Robertson-Walker-like (FLRW) coordinates and struggling with cosmology, which is beyond the scope of this thesis.

The anti-de Sitter spacetime does not possess such horizon. This thesis will not deal with the AdS metric, but with the dS metric when discussing regular Black Hole cores in section 3.4.

### 1.3 Higher dimensional Gravity

From the mathematical/geometrical viewpoint, in terms of tensor calculus, the generalization from 4 to  $d$  space-time dimensions is trivial: One can write the Einstein equations in  $d$  space-time dimensions as

$$R_{MN} - \frac{1}{2}g_{MN}R = -8\pi G T_{MN} \quad (1.24)$$

with capital latin indices (like  $A, B, M, N$ ) running from  $0, 1, \dots, d-1$  while the lower greek indices (like  $\alpha, \beta, \mu, \nu$ ) indicing the 4d submanifold from  $0, \dots, 3$  and the lower latin indices (like  $a, b, m, n$ ) indicing the 3d spatial submanifold as before from  $1, \dots, 3$ . Without indices, bold vectors (like  $\mathbf{x}, \mathbf{y}$ ) shall indicate  $d$ -dimensional vectors, while vectors with arrow (like  $\vec{x}, \vec{y}$ ) indicate  $(d-1)$ -dimensional vectors (just the spatial part in a given metric).

Black holes in higher dimensions are more diverse than in 4d, since more topologies are possible [24], for example ring solutions (“black rings”, like donuts). The most simple generalization of the Schwarzschild solution to  $d$  dimensions is the *Schwarzschild-Tangherlini* metric with line element

$$ds^2 = (1 - V(r))dt^2 - (1 - V(r))^{-1}dr^2 + r^{2+n}d\Omega_{2+n}^2. \quad (1.25)$$

and gravitational potential

$$V(r) = \frac{2}{n+2} \frac{M}{M_*^{2+n}} \frac{1}{r^{1+n}}. \quad (1.26)$$

The density is given by

$$\rho(\mathbf{x}) = \frac{M}{\Omega_{2+n} r^{2+n}} \delta^{1+n}(\mathbf{x}), \quad (1.27)$$

and makes use of the higher dimensional delta function  $\delta^d$  and the surface  $\Omega_{2+n}$ . This will be the basis for modifications in section 2.5.2.

In this section, popular higher dimensional theories are introduced that motivate to do research on higher dimensional Black Holes. Kaluza Klein and Randall-Sundrum theory is only mentioned briefly, the focus will be on the ADD-model, which forms the basis for all Black holes Discussed in this thesis.

### 1.3.1 Kaluza Klein theory

Extending gravity for higher dimensions has a long standing history, first suggestions go back to Nordström and Kaluza [30] and propose using extra dimensions for unification of gravity and electromagnetism. In 1921, this lead to Kaluza Klein theory, where Kaluza introduced one space-like extradimension and a scalar field  $\phi$  (corresponding to a new particle). KK theory is capable of producing both Einstein field equations and Maxwell equations at once. This works out with any four dimensional metric  $g_{\mu\nu}$  which is put in the five dimensional extension according to

$$g_{MN} = \begin{bmatrix} g_{\mu\nu} e^{\phi/\sqrt{3}} + e^{-\phi^2} A_\mu A_\nu & e^{-\phi^2} A_\nu \\ e^{-\phi^2} A_\mu & e^{-\phi^2} \end{bmatrix}. \quad (1.28)$$

The Einstein field equations (1.24) for  $d = 5$  are a system of 25 equations that decouple to the ordinary 4d Einstein equations with a modified (effective) 4d energy momentum tensor  $\tilde{T}_{\mu\nu}$ ,

$$R_{\mu\nu} - \frac{1}{2}g_{\mu\nu}R = -8\pi G\tilde{T}_{\mu\nu}, \quad \text{with } \tilde{T}_{\mu\nu} = \frac{1}{4}e^{-\sqrt{3}\phi}F_{\mu\sigma}F_\nu^\sigma + \frac{\partial_\mu\phi\partial_\nu\phi}{2}, \quad (1.29)$$

the Maxwell's equations for the field  $A_\mu$ ,

$$\partial_\mu\partial^\nu A^\mu - \partial_\mu\partial^\mu A^\nu = 0 \quad (1.30)$$

and a relativistic equation for the scalar field  $\phi$

$$\partial_\mu\partial^\mu\phi = \frac{-\sqrt{3}}{4}e^{-\sqrt{3}\phi}F_{\mu\nu}F^{\mu\nu}. \quad (1.31)$$

Note that in this theory, the gravitational coupling constant  $G$  remained untouched. The fifth dimension is supposed to be compactified on *microscopical* scales (cf. figure 1.2).

### 1.3.2 Randall-Sundrum scenario

The Randall-Sundrum (RS) model was proposed in 1999 and also implies the existence of one large spatial extra dimension. In contrast to KK, the fifth dimension has constant negative curvature (AdS). The five dimensional line element is given by [38]

$$ds^2 = e^{-2kr_c|y|}g_{\mu\nu}dx^\mu dx^\nu + r_c^2 dy^2 \quad (1.32)$$

with  $g_{\mu\nu}$  the 4d space time,  $k \sim 1/L_*^2$  a parameter of the order of the fundamental Planck scale,  $y$  the extra coordinate and  $r_c$  the compactification radius of the extra dimension. The RS metric can be derived like KK from the 5d EFEs with negative cosmological constant.

The RS (and KK) scenario are mentioned only for the sake of completeness and to show alternatives to the following ADD model which is the first one proposing *large* extra dimensions. Historically, the RS model is one year younger than the ADD model and also addresses the Hierarchy Problem by giving rise to an effective 4d Planck mass

$$M_{Pl}^2 = (1 - e^{-2kr_c})M_*^3/k. \quad (1.33)$$

The deviation and discussion of the model is beyond the scope of this work. See e.g. [38] for a review in the context of micro Black Holes.

### 1.3.3 ADD-model and Large Extra Dimensions

In 1998, Nima Arkani-Hamed, Savas Dimopoulos and Gia Dvali (ADD) proposed a model with  $n$  large spatial extra dimensions (LXDs or LEDs). This model lives in a  $d = 4 + n$  dimensional space-time. The observable four-dimensional universe is called the *brane* (the term comes from membrane), embedded in the higher-dimensional *bulk*. These  $n$  extra dimensions are taken to be flat and compactified, like the extra dimension in the KK theory, but the compactification radius  $R_c$  is considered *large* compared to

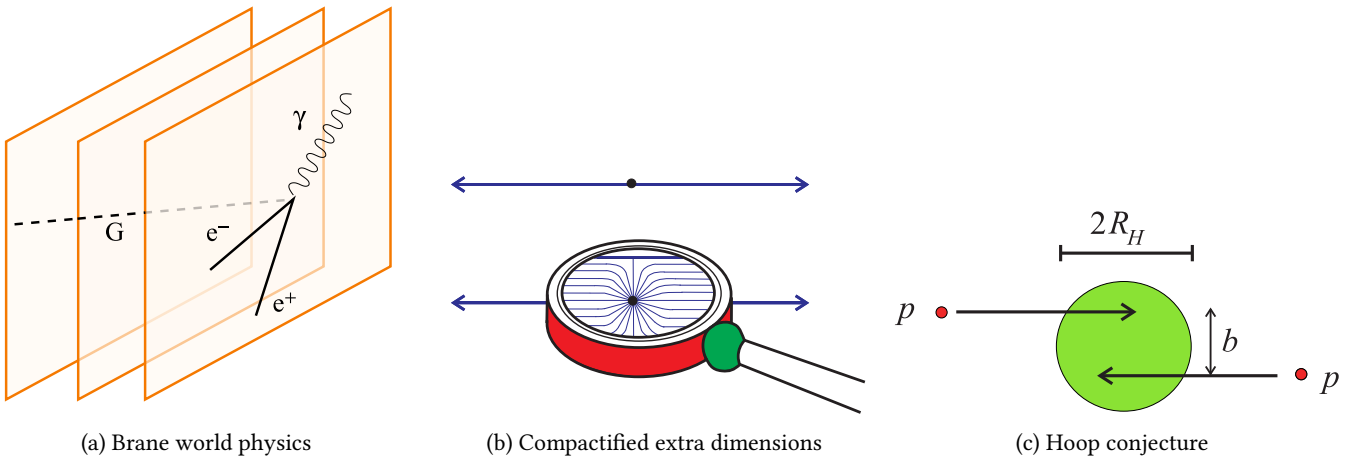


Figure 1.2: Illustrations on how to imagine large extra dimensions and brane world physics. The (orange) 4d branes are displayed as 2d surfaces, while one extra dimension is displayed horizontally. While the QED process takes place on the brane, and neither electron, positron and photon can escape the brane, the graviton is allowed to freely traverse the whole space-time.

The compactification picture (b) shows where one faces extra dimensions even in real life: When zooming in, the one dimensional horizontal line shows a vertical substructure.

The hoop conjecture illustrations (c) shows how to imagine a particle collision with impact parameter  $b < 2R_H = 2L_*$ . Pictures taken and modified from [16, 33, 43].

the Planck length. Typical values are  $R_c \approx 1\text{mm}$ . This is small enough to agree with non-observed deviations from Newton's law. The idea of the ADD model is, that all Standard Model fields *live* on the brane, that is, do not notice the existence of more than four dimensions. Only gravitons and possibly scalar fields [37] are allowed to propagate everywhere (bulk and brane). It is hard to imagine such concepts. See therefore figure 1.2a for a way to imagine brane and bulk space, while figure 1.2b displays a way to imagine compactified extra dimensions.

The large extra dimension scenario can solve the weak hierarchy problem of the Standard Model by imposing a new fundamental mass scale  $M_*$  which produces the observable 4d Planck mass scale  $M_{\text{Pl}}$  by integrating out the volume of the extra dimensions. The weak hierarchy problem is the strange fact that the electro-weak energy scale (masses of electro-weak gauge bosons) is about  $10^{32}$  times smaller than the gravity energy scale (Planck mass). In other formulations, it is the question why the Higgs boson is so much lighter than  $M_{\text{Pl}}$ . The extra dimensional outcome states that one can see only an effective weak coupling constant  $G = 1/M_{\text{Pl}}^2$ , because it is the result of the integrated out volume of the extra dimensions, where gravity also propagates. This ratio is defined as

$$M_{\text{Pl}}^2 = C_n V_n M_*^{n+2}, \quad (1.34)$$

with  $V_n$  the volume of the enrolled extra dimensions, with tori and compactification radii  $R_c$  e.g.  $V_n = (2\pi R_c)^n$  and a dimensionless prefactor  $C_n = \mathcal{O}(1)$ .

Note that there are multiple conventions about the prefactor  $C_n$  in (1.34). Here it is chosen most like the Han-Lyken-Zhang notation (HLZ), as proposed in the appendix of [16]:

$$C_n = \left( \frac{\Omega_{n+2}}{\Omega_2} \right)^{\frac{1}{n+2}} \quad (1.35)$$

The prefactor  $C_n$  is used to compensate higher dimensional numerical contributions from volume integrals. Without extra dimensions ( $n = 0$ ),  $M_{\text{Pl}} = M_*$ .

In the ADD scenario, these extra dimensions were to be meant *large* in extend, that is, in the millimeter scale. Thus, the fundamental coupling reaches the TeV scale even with one extra dimension. This opens the door for experimental tests, as the center of mass energy of the Large Hadron Collider (LHC) at cern is in the same order of magnitude (10 TeV).

### 1.3.4 Black Holes in particle detectors

Quantum Black Hole formation in particle detectors is usually assumed by super-Planckian particle collision processes (Hoop conjecture). In such a process with a center of mass energy in the order of the (fundamental) Planck mass and a impact parameter (cross section estimation) in the order of the (fundamental) Planck length, enough matter is compressed to form an event horizon of quantum size. This experimental signature is the main motivation for investigating Black Holes in large extra dimensions.

For literature about the experimental setup and observation of Black Holes in particle accelerators like the LHC, see e.g. [8, 9, 16, 37, 38, 43, 54].

# Chapter 2

## Short-scale improved Black Holes

This section emphasizes the breakdown of General Relativity at quantum scales (the Planck scale) and gives an overview about theories trying to cure the ultra violet behaviour. Requirements for a final state spherically symmetric UV improved model are formulated and fulfilling metrics are derived.

### 2.1 Black hole evaporation phases

Mini Black Holes that can be produced e.g. in particle detectors like discussed in the last section evaporate by Hawking radiation. This process is typically categorized in four phases [9, 33, 43]:

- **Balding phase.** In this phase the Black Hole loses the *hair* which consists of asymmetries (multipole moments) and gauge field hair.
- **Spin down phase.** The Black Hole radiates away all of its angular momentum and some mass.
- **Schwarzschild phase.** The Black Hole is spherical and still radiates.
- **Planck phase.** The Black Hole mass reaches the Planck mass and quantum gravity effects get strong.

Figure 2.1 illustrates these phases.

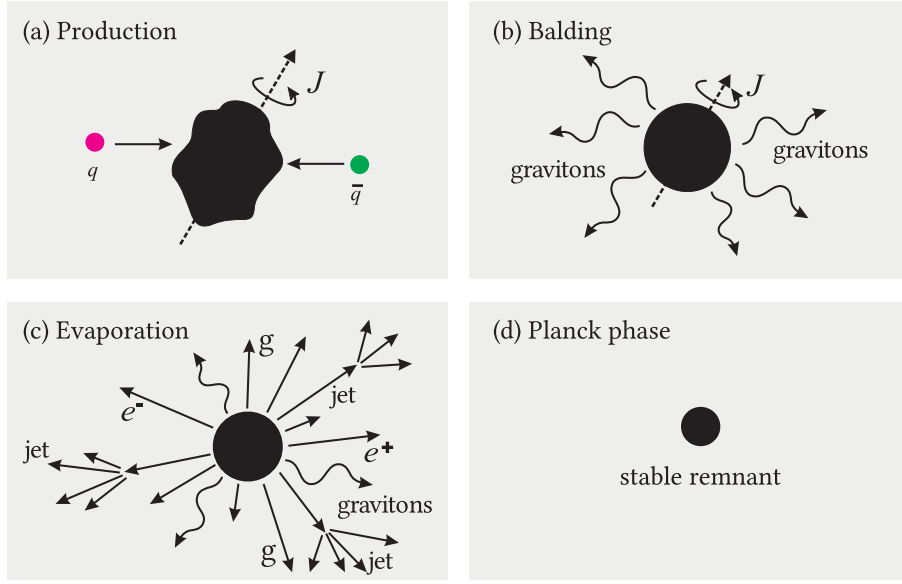


Figure 2.1: Sketch of the evaporation phases of a quantum Black Hole produced in a particle accelerator: (a) Production as described in section 1.3.4, (b) Balding phase, (c) Spin down and Schwarzschild phase and (d) Planck phase. Figure modified from [33].

## 2.2 Problems of the Schwarzschild Black Hole

One of the tenets of High Energy Physics is the association of the failure of a theory at scales where the theory predicts singularities. It is common belief that nature is nonsingular in the same way (classical) physics is supposed to be “smooth” everywhere. Against this backdrop, the obvious problem of the Schwarzschild Black Hole is the curvature singularity in the origin which may be traced to the Dirac delta distribution composing the matter source  $\delta(\mathbf{x})$ . Anyway, the Dirac delta may be seen as an idealization, so this may be casted as a philosophical problem.

Actually the real flaws occur at Black Hole thermodynamics. The Hawking temperature for Black Holes is defined by the surface gravity  $\kappa = \partial_r g_{00}|_{r_H}$  by

$$T_H = \frac{\hbar\kappa}{2\pi} = \frac{\hbar}{8\pi GM}. \quad (2.1)$$

Assuming energy loss when a Black Hole radiates, the evaporating Black Hole gets hotter and hotter and the picture breaks down when  $T \sim M$ , that is, when the emission occurs at a temperature of the order of the Black Hole mass.

Based on this temperature, the Black Hole thermodynamics are constructed. The Schwarzschild heat capacity  $C_T = dM/dT$  is negative and approaches asymptotically zero for increasing temperatures. Frolov therefore calls Schwarzschild thermodynamics *ill defined*, since such a Black hole cannot be in a stable equilibrium with a surrounding heat bath [27].

Despite the obvious fundamental contradictions between General Relativity and Quantum Mechanics, at shortest scales there is even a tangible particle-Black Hole *duality*, illustrated in figure (2.2a). On the quantum mechanical side, each particle with mass (=energy)  $m$  can be assigned a length scale. This can be the Compton wavelength  $\lambda_C = \hbar/mc$ , so  $L_{\text{particle}} \sim 1/m$ , as the red curve indicates (The mass  $m$  for a particle with  $v = c$  is just  $m = pc^2$ ). On the other hand, the Black hole picture assigns each mass distribution a length by means of the Schwarzschild event horizon  $r_H = 2GM/c^2$ , so  $L_{\text{Black hole}} \sim m$ , as the blue curve indicates. These two curves cross at the Planck scale  $L_{\text{particle}} = L_{\text{Black hole}} = \sqrt{\hbar c/G} := L_{\text{Pl}}$  (numerical factors are suppressed in this picture). Let’s trace as a gedankenexperiment a particle in an accelerator where its energy (velocity) is increased, resulting in a better length scale resolution (particle compression, red arrow). At the Planck scale  $M_{\text{Pl}}$ , suddenly the *hoop conjecture* expects the particle to

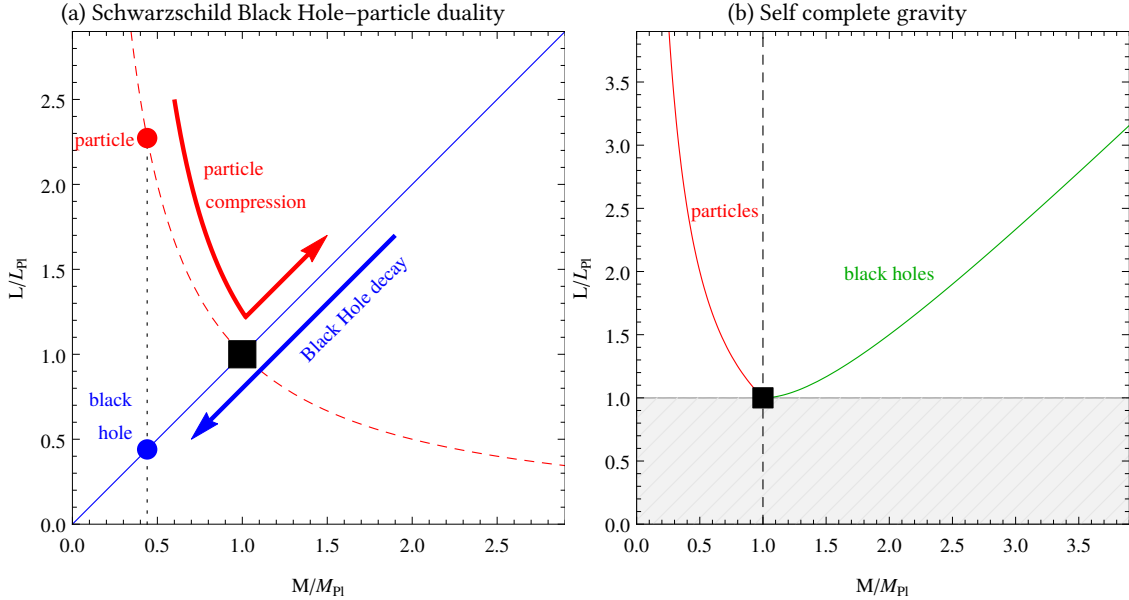


Figure 2.2: Length-vs-Mass pictures, see main text for description

become a Black Hole, and further (fictive) acceleration increases the size of the object again. Now one can turn off the accelerator, and by Hawking evaporation the Black Hole decays (blue arrow). As there is no *inverse hoop conjecture* in particle physics, nothing prevents the Schwarzschild Black Hole from evaporating below the Planck scale. Suddenly, one ends up with a situation where two theories predict two different sizes for the same system. Which one is correct?

There are two ways out of this awkward situation: Either General Relativity breaks down and must be replaced by a completely different theory, or it can be saved by some kind of *completeness*. In figure 2.2b a solution is sketched: By modifying the gravitational event horizon in a way that it smoothly merges into the particle picture, one gets a unique particle–Black Hole interpretation and a *minimum length scale* of physics  $L_{Pl}$ . In this theory, there is literally no way to probe distances below  $L_{Pl}$  as it is either circumvented by quantum mechanical uncertainty or Black Hole production.

## 2.3 Quantum Gravity Black Holes

This section gives a two-page overview about Black Holes in different Quantum Gravity approaches and their relationship to this work. It primarily follows the “six families of Black Holes” proposed in [58] and closes with *String theory*, which is certainly the most popular candidate for QG.

### Non-local gravity Black Holes

In this category of approaches, the starting point is a nonlocal field theory by means of a nonlocal contribution to the geometric part of the Einstein field equations. In [49], this is done with a derivation operator acting on the Einstein tensor in a way that

$$\mathcal{F}^{-2}(\square(x)/\Lambda_G^2) \left( R_{\mu\nu} - \frac{1}{2}g_{\mu\nu}R \right) = 8\pi G_N T_{\mu\nu}. \quad (2.2)$$

This goes back to nonlocal action modifications in gravity proposed by Barvinsky (see [6] for a recent review and [5] for a more comprehensive early work). Actually, such an approach is also used for curing divergences at perturbative expansion of the Einstein-Hilbert action up to a super-renormalizable theory of Quantum Gravity [48].

In the last chapter 5 of this thesis, nonlocal operators  $\mathcal{F}^{-2}$  are discussed in spite of finding a dual theory to a quantum matter density.

### Noncommutative Black Holes

Noncommutative geometry suggests a “fuzzy” spacetime by imposing a commutation relation on the quantum-mechanical position operator  $\mathbf{x}^\mu$ . In terms, this reads

$$[\mathbf{x}^\mu, \mathbf{x}^\nu] = i\theta^{\mu\nu} \quad (2.3)$$

with the matrix  $\theta^{\mu\nu}\theta > 0$  imposing the “discretization” of space-time. This idea leads to a space-time uncertainty and finally to a gaussian energy density approach as dirac replacement in the noncommutative inspired Schwarzschild solution,

$$\rho_\theta(r) = \frac{M}{(4\pi\theta)^{3/2}} e^{-r^2/4\theta}. \quad (2.4)$$

From this equation one can read that  $r \sim \sqrt{\theta}$  corresponds to the length scale where noncommutative effects get strong. Funny enough, the metric produced by (2.4) possesses a regular core like the one we will contrive in this chapter [55].

A in-depth review about Noncommutative Black Holes is [51]. The first extradimensional extension from Rizzo 2005 [63] actually determines the syntax and conventions used in this thesis.

### Generalized Uncertainty Principle Black Holes

The generalized uncertainty principle is perhaps the closest approach to create a “matching” picture 2.2b. It can be formulated by suggesting as well a modified Compton scale as a generalized event horizon [11,12] and states, in the simplest form

$$\Delta x \Delta p \geq \frac{\hbar}{2} (1 + \alpha x^2 + \beta p^2). \quad (2.5)$$

Note that for  $\alpha = \beta = 0$ , this is the Heisenberg uncertainty principle. By means of a Hilbert space representation [39], for  $\alpha = 0$  on can deduce a modified momentum integration measure where  $p \sim \sqrt{\beta}$  plays the role of a high energy regulator, and this can be used to compute the GUP-Schwarzschild Black Hole with energy density [35,36]

$$\rho_\beta(r) = \frac{M}{(2\pi)^3} \int \frac{d^3p}{1 + \beta p^2} e^{i\mathbf{x} \cdot \mathbf{p}}. \quad (2.6)$$

Surprisingly, there also is a link to this thesis: Densities like (2.6) have been extended to higher dimensions [44], and the integration technique to solve nonlocal operators introduced in chapter 5 turned out to be successful to compute fourier transformations of GUP operators.

### Loop Quantum Black Holes

Loop Quantum Gravity (LQG) is the competitor for String Theory that has the major advantage of preserving *background-independence*, as this is a major pillar of General Relativity. Therefore, LQG cannot be a perturbative expansion of Quantum GR by means of  $\tilde{g}_{\mu\nu} = g_{\mu\nu} + h_{\mu\nu}$ , since this would distinguish a special fixed classical background metric  $g_{\mu\nu}$ . The main principle in LQG is general covariance paired with quantum principles. Contemporary formulations use a graph as basic principle, a network (the “foam”) with spacetime points as vertices and a discrete minimal length distance as edges and therefore refined the building word *loop* QG. According to Ashtekar, “loops play no essential role in the theory now, for historical reasons, this name is widely used”; there lies the close relationship to lattice gauge theories, as closed loops resemble Wilson plaquettes [64,74].

It is a long way from Loop Quantum Gravity to Loop Quantum Black Holes (LQBHs), and contemporary research about LQBHs is fairly less “descriptive” than the Black Holes modified by the principled

mentioned before. See e.g. Modesto [47] who, amongst other things, finds out after a lengthy calculation that the Schwarzschild curvature singularity is no more present in LQBH.

Note that a particularly significant result is a fundamental explanation of the Black Hole logarithmic entropy correction that was predicted by Wilson. The logarithmic Black Hole entropy term will be discussed in depth in section 4.4.

See the texts of Thiemann [72, 73] and Ashtekar [2] for a pedagogical review about LQG. For a pedagogical introduction with focus on spin foams, see [61].

### Asymptotically safe gravity Black Holes

Asymptotically safe gravity is built on a running coupling  $G(k)$  which is the result of renormalization group treatments; general covariance is maintained with this approach. The basic idea is to make gravity an effective theory at momentum scale  $k$  and therefore be safely able to do physics with momenta  $k' \gg k$ .

Applied to Black Holes,  $G(r)$  takes the place of Newton's constant in the Schwarzschild metric [25]. Thus it is possible to get Black Hole remnants that resemble the holographic profile we encounter in the next sections.

For introductory papers, see e.g. Reuter [10, 62] and the review [59] by the same author.

### Black holes in String Theory

String Theory is the theory of quantum-mechanical relativistic one-dimensional “vibring strings” (like waves), and according to the popular picture, different excitation energies correspond to different point-like particles postulated by the standard model of particle physics. The term “String Theory” is usually used similarly to superString Theory, that is, String Theory including supersymmetry (SUSY, a symmetry that relates each boson to its superpartner, the fermion, and vice versa). The existence of extra dimensions, as introduced in section 1.3, is actually predicted by String Theory. String Theory is most criticised because its large number of solutions and especially because the dependence on a background spacetime which explicitly breaks general covariance. On the other hand, String Theory only needs one fundamental minimal length scale  $\ell_0$  and may be treated perturbatively.

Considering Black Holes, String Theory is especially able to make statements about extremal Black Hole situations, as we will encounter in the next chapter. The enticing recast of an extremal Black Hole as a *particle* is unique to String Theory. String Theory also predicts a logarithmic entropy correction as LQG does.

String Theory is handled e.g. in the book of Kiefer [41], Black Holes in String Theory are discussed in [45]. Probably a good closing overview over all approaches gives the review article [40].

## 2.4 Requirements for self-complete Black Hole metrics

The following three properties for short-scale improved Black holes were proposed in [56]. They imply the newly developed theory is equipped with a *characteristic length scale*  $l_0$  which is, of course, associated with an energy scale  $1/l_0$  of theory validity.

1. A *regular Black Hole* that has no more curvature (Ricci scalar) singularity at the origin, in terms

$$R(0) < \infty. \quad (2.7)$$

2. *Classical low-energy limit*, that is, Schwarzschild behaviour of the metric for big distances, in terms

$$g_{00}(r) = 1 - \frac{2GM}{r} \quad \text{for } r \gtrsim l_0. \quad (2.8)$$

3. *Self-encoding* of the characteristic minimal length scale  $l_0$  in the radius of the *extremal* configuration  $r_0$ , that is,

$$l_0 = r_0. \quad (2.9)$$

This third requirement is crucial: Self-encoding enables  $l_0$  being the only *universal scale*, as the theory requires no new length scale like  $\sqrt{\beta}$  from GUP,  $\theta$  from NCG or  $\ell_0$  from String Theory.

## 2.5 Quasi-classical source terms

### 2.5.1 Derivation of the metric

In this section, the metric for a potential  $V(r)$  that behaves like the Schwarzschild potential  $V(r) = 2GM/r$  at large  $r$  is described. The notation follows [63].

The starting point is a static isotropic matter density  $\rho(r)$  with  $\lim_{r \rightarrow \infty} \rho(r) = 0$ . The ansatz for the solution is the  $d = n + 4$  dimensional spherical symmetric and static metric

$$ds^2 = -e^{\nu(r)} dt^2 + e^{-\nu(r)} dr^2 + r^2 d\Omega_{n+2}^2 \quad (2.10)$$

$$= -(1 - V(r)) dt^2 + (1 - V(r))^{-1} dr^2 + r^2 d\Omega_{n+2}^2 \quad (2.11)$$

with  $\Omega_{n+2}$  the surface line element of an  $(n + 3)$  sphere (for details about the surface sphere, see appendix 5.2.2). The spherical coordinates are given by  $x_\mu = (x_0, \vec{x}) = (x_0, r, \phi, \theta_1, \dots, \theta_{n+2})$ , but it is written  $i$  instead of  $\theta_i$  ( $i = 1, \dots, m$  and  $m := n + 2$ ) in the indices to improve readability, referring to the diagonal coefficients in the metric as

$$g_{AB} = \text{diag}(g_{00}(r), -g_{00}^{-1}(r), g_{\phi\phi}(r, \phi), g_{11}(r, \theta_1), \dots, g_{mm}(r, \theta_m)) \quad (2.12)$$

The argumentation follows the derivation of the inner Schwarzschild solution, as can be found in General Relativity textbooks: The property  $-g_{00} = g_{11}^{-1}$  is required for flat space at large distances.

Given the matter density and the metric ansatz, the stress tensor  $T^{NM}$  can be determined. Due to the symmetry of the problem, it can already be stated as

$$T_N^M = \text{diag}\left(T_0^0, T_r^r, T_\phi^\phi, T_1^1, T_2^2, \dots, T_m^m\right) = \text{diag}(\rho, \rho, p, p, \dots, p), \quad (2.13)$$

following [55, 63]. Now switching to  $(1, 1)$  tensor form yields the conservation of energy equation as  $\nabla_N T_M^N = 0$  with

$$T_B^A = g_{BC} T^{AC} = g_{BB} T^{AB} = \text{diag}(g_{00} T^{00}, g_{rr} T^{rr}, \dots, g_{mm} T^{mm}). \quad (2.14)$$

One can see that only the equation with index  $M = r$  contributes new information. In order to solve the equation (no sum convention here)

$$0 = \nabla_0 T_r^0 + \nabla_r T_r^r + \sum_i \nabla_i T_r^i, \quad (2.15)$$

the covariant derivatives derivative  $\nabla_N$  and Christoffel symbol  $\Gamma_{AB}^C$  must be computed (see appendix 5.2.2 for the definitions). The summands of (2.15) are given by

$$\nabla_0 T_r^0 = \partial_0 T_r^0 + \Gamma_{0D}^0 T_r^D - \Gamma_{0r}^D T_D^0 = \frac{1}{2} g^{00} T_r^r \partial_r g_{tt} + \frac{1}{2} g^{00} T_0^0 \partial_r g_{tt} \quad (2.16a)$$

$$\nabla_r T_r^r = \partial_r T_r^r + \Gamma_{rD}^r T_r^D - \Gamma_{rr}^D T_D^r = \partial_r T_r^r \quad (2.16b)$$

$$\forall i : \quad \nabla_i T_r^i = \partial_i T_r^i + \Gamma_{iD}^i T_r^D - \Gamma_{0r}^D T_D^i = \frac{1}{2} g^{ii} T_r^r \partial_r g_{ii} + \frac{1}{2} g^{ii} T_0^0 \partial_r g_{ii} \quad (2.16c)$$

One ends up with the explicit equation

$$0 = \partial_r T_r^r + \frac{1}{2} g^{00} (T_r^r - T_0^0) \partial_r g_{00} + \frac{1}{2} \sum_i g^{ii} (T_r^r - T_i^i) \partial_r g_{ii} \quad (2.17)$$

Now plugging in the ansatz for  $T_B^A$ , the term  $(T_r^r - T_0^0)$  vanishes. For all angles, the term

$$g^{ii} \partial_r g_{ii} = \frac{1}{r^2 \sin^j(\theta_j)} \partial_r (r^2 \sin^j(\theta_j)) = \frac{2}{r} \quad (2.18)$$

is the same and thus all remaining energy momentum components are determined to

$$T_i^i = T_0^0 + \frac{r}{n+2} \partial_r T_0^0 = \rho + \frac{r}{n+2} \partial_r \rho. \quad (2.19)$$

In order to solve the Einstein equation, in addition to the energy momentum tensor one needs the Ricci tensor as additional ingredient. It is given as the contraction of the Riemann tensor

$$R_{\mu\nu} = \partial_\lambda \Gamma_{\nu\mu}^\lambda - \partial_\nu \Gamma_{\lambda\mu}^\lambda + \Gamma_{\mu\gamma}^\lambda \Gamma_{\nu\mu}^\gamma - \Gamma_{\nu\gamma}^\lambda \Gamma_{\lambda\mu}^\gamma, \quad (2.20)$$

see Appendix 5.2.2 for the values of all Christoffel symbols. The Ricci tensor is again diagonal, with the entries

$$R_0^0 = R_r^r = -\frac{e^\nu}{2} \left( \partial_r^2 \nu + (\partial_r \nu)^2 + (n+2) \frac{\partial_r \nu}{r} \right) = \frac{1}{2} V''(r) - \frac{n+2}{2} \frac{V'(r)}{r} \quad (2.21a)$$

$$\forall i : \quad R_i^i = \frac{1+n-e^\nu (1+n+r\partial_r \nu)}{r^2} = (1+n) \frac{V(r)}{r^2} + \frac{V'(r)}{r}. \quad (2.21b)$$

The Ricci scalar is then given by

$$R = R_N^N = \frac{(n+2)V(r)}{r^2} + V''(r) \quad (2.22)$$

Now one can write out the Einstein equations in a trace reversed form, in  $(1, 1)$  tensor notation for  $d$  dimensions:

$$R_A^B = \frac{1}{M_*^{n+2}} \left( T_A^B - \delta_A^B \frac{T_C^C}{n+2} \right) \quad (2.23)$$

Since  $R, T, \delta$  are diagonal, the Einstein equations reduce to  $d$  non-zero equations where finally only two equations differ from each other, identified by their indexes  $A, B = r, r$  and  $A, B = i, i$ . The later one gives the following first order differential equation for  $V(r)$ :

$$V'(r) + \frac{n+1}{r} V(r) = \frac{1}{M_*^{n+2}} \frac{r\rho(r)}{n+2} \quad (2.24)$$

The general solution of the metric for any  $\rho(r)$  is given by the integral

$$V(r) = \frac{1}{r^{n+1}} \left( \frac{1}{(n+2)M_*^{n+2}} \int_{c_1}^r x^{n+2} \rho(x) dx + c_2 \right) \quad \text{with } c_1, c_2 = \text{const} \quad (2.25)$$

The boundary values  $V(0)$  and  $V'(0)$  give rise to the two integration constants  $c_1$  and  $c_2$ . Physically, they allow the low-energy matching of the theory. In the context of this thesis,  $c_1$  is important for discussion about minimal lengths.

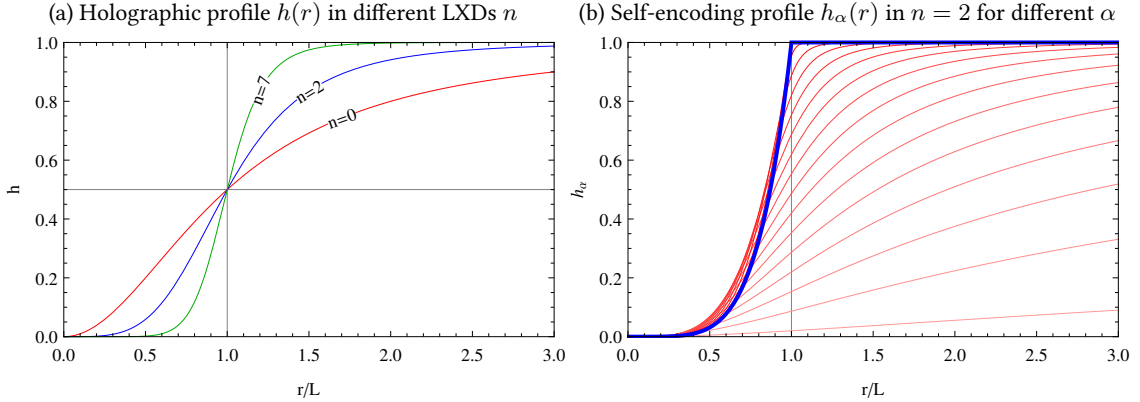


Figure 2.3: The two chosen Heaviside step function smearing functions with their characteristic behaviour, each scaled against their built in length scales  $\tilde{r}_0$ . For more details see Appendix 5.2.2.

### 2.5.2 Smeared matter density

Starting with the Schwarzschild-Tangherlini point-like static and spherically symmetric density

$$\rho(r) = \frac{M}{\Omega_{n+2} r^{n+2}} \delta(r). \quad (2.26)$$

The Dirac delta  $\rho(r)$  is replaced by a smeared version which we define as the derivative  $\frac{d\Theta(r)}{dr} = \delta(r)$  of the Heaviside unit step function

$$\Theta(r) = \begin{cases} 0 & \text{when } r < 0 \\ 1 & \text{when } r \geq 0 \end{cases}. \quad (2.27)$$

The generic *Schwarzschild-like* energy density is therefore chosen as

$$\rho(r) = \frac{M}{\Omega_{n+2} r^{n+2}} \frac{dH(r)}{dr}, \quad (2.28)$$

which, when inserting into the integral 2.25, gives us the generic metric, for a given  $H(r)$ , as

$$V(r) = \frac{1}{2+n} \frac{M}{M_*^{n+2}} \frac{H(r)}{r^{n+1}}. \quad (2.29)$$

A closer discussion about the physical meaning of the mass parameter  $M$  will be given in section 3.1.

## 2.6 Choices for mass profiles and their $d$ -dimensional extension

In the paper of Nicolini and Spallucci about holographic screens in UV self complete gravity [56], there are two mass profiles presented which will be referred to in this work as

$$\text{the } \textit{holographic} \text{ profile} \quad h(r) = \frac{r^2}{r^2 + \tilde{r}_0^2}. \quad (2.30a)$$

$$\text{the } \textit{self-regular} \text{ profile} \quad h_\alpha(r) = \frac{r^3}{(r^\alpha + \tilde{r}_0^\alpha/2)^{3/\alpha}} \quad \text{and} \quad (2.30b)$$

Each of them builds a matter density and thus a space-time by plugging  $H \in \{h_\alpha, h\}$  into the matter density (2.28).

Note that these profiles are just invented from nothing, that is, they are an *educated guess* or *ab-initio*, to solve the problems they are confronted with on the next pages. The special feature of the main paper of this thesis [56] is that *there is no further ingredient than General Relativity*. There is no need to stress a more advanced theory like String Theory or loop quantum theory to produce the densities (2.28) in the limit. But these profiles do not only produce *toy models* but have profound physical properties that are uncovered in the next two chapters. The naming will become clear: While the *self-regular* profile fulfills all requirements 1-3 from section 2.4, especially the regularity, the holographic one is not regular, but features logarithmic corrections to the Black Hole entropy, as will be seen in section 4.4.

### 2.6.1 Extension to extra dimensions

In this work, the properties of Black Holes of the profiles extended to  $n$  large extra dimensions are investigated. It turns out that the correct choice is

$$h(r) = \frac{r^{2+n}}{r^{2+n} + \tilde{r}_0^{2+n}} \quad \text{and} \quad h_\alpha(r) = \frac{r^{3+n}}{(r^\alpha + \tilde{r}_0^\alpha/2)^{\frac{3+n}{\alpha}}}. \quad (2.31, 2.32)$$

With  $n \rightarrow 0$ , they reduce to the 4-dimensional models used in [56].

It may be denoted that these choices were “guessed”, as every  $2 \rightarrow 2+n$  or  $3 \rightarrow 3+n$  in a “natural” manner. The choice for the holographic model is justified by yielding the required entropic corrections, as shown in section 4.4. For the self-encoding model, where the hell is the motivation?

### 2.6.2 Length scales

Before heading to the physical properties of Black Holes created by such mass profiles, one should shortly sum up the new variables introduced by those profiles: In both cases, it is a length scale  $\tilde{r}_0$  that plays the role of the *width* of the delta/heaviside approximation, as the variance  $\sigma$  in the well-known Gaussian approximation

$$\delta_\sigma(r) = \frac{1}{\sqrt{2\pi}\sigma} \exp\left(-\frac{r^2}{2\sigma}\right), \quad \delta(r) = \lim_{\sigma \rightarrow 0} \delta_\sigma(r). \quad (2.33)$$

Figure 2.3 displays the two profiles rescaled to their length scale  $\tilde{r}_0$ . For the holographic profile,  $\tilde{r}_0$  is a kind of “half-life scale”, as  $h(\tilde{r}_0) = 1/2$ , for the self-encoding one it is  $h_\alpha(\tilde{r}_0) = (3/2)^{-\frac{3+n}{\alpha}}$ . Figure 2.3a shows that increasing  $n$  create a sharper distribution. As a comment, note that for  $n \rightarrow \infty$ , the curve resembles a displaced step function  $h_{n \rightarrow \infty}(r) = \Theta(r - \tilde{r}_0)$ . This reflects the fact that all volume in a  $\infty$ -sphere lives on the surface.

Figure 2.3b looks basically the same in any dimension, but shows how the additional degree of freedom  $\alpha$  modify the distribution. Bigger  $\alpha$  create a sharper curve until the limit  $\alpha \rightarrow \infty$  where the difference between  $h(r)$  and  $h_\alpha(r)$  clearly stands out: The additional degree of freedom can be used for a  $h_\infty(r) \sim r^{3+n}$  behaviour for  $r < \tilde{r}_0$  while  $h_\infty(r) = 1$  for  $r > \tilde{r}_0$ .

Note that until now,  $\tilde{r}_0$  and  $\alpha$  have no physical meaning, they are just mathematical constants. Linking  $\tilde{r}_0$  according to the self-encoding principle (2.9) to a physical length scale  $l_0$  is the agenda for the next chapter.

### 2.6.3 The Schwarzschild limit

In the next sections, the properties of the class of  $\Theta(r) \rightarrow H(r)$  smeared Black Holes are discussed. For comparison, it will frequently be useful to take back the limit  $H(r) \rightarrow \Theta(r)$ . To do so mathematically correct, one examines the limit of the regulator  $\tilde{r}_0 \rightarrow 0$ . Thus, it will be (only) safe for  $r > 0$  to replace any occurrence of

$$H(r) \rightarrow 1, H'(r) \rightarrow 0, H''(r) \rightarrow 0, \dots \quad (2.34)$$

according to the finite values  $\Theta(r) = 1$  and  $\delta(r) = 0$  for  $r > 0$ . This of course also holds for products like  $H(r)H'(r) \rightarrow 0$ . Interestingly, this naive approach is also doable at  $r = 0$ , but one may not expect this would give statements of divergence behaviour.

# Chapter 3

## Geometry of the Black Holes

In this chapter, the geometry and conformal structure of the family of Black Hole geometries presented in the previous chapter is discussed. This will lead to the discussion about the special features of regular Black Holes.

### 3.1 The Mass

The mass contained inside a  $(3+n)$ -sphere (the object will be referred to as  $\mathcal{B}(r)$ ) with radius  $r$  is given by the integral

$$m(r) = \int_{\mathcal{B}(r)} \rho(x) d^{n+3}x = M \int_0^r H'(r) dr = MH(r). \quad (3.1)$$

From the mathematical viewpoint, the mass  $M$  is just a constant that may be used to fulfill the horizon equation  $V(r) = 1$ . Therefore I set

$$M = (n+2)M_*^{n+2} \frac{r_H^{n+1}}{H(r_H)}, \quad (3.2)$$

so when plugging into the metric

$$V(r) = \frac{1}{n+2} \frac{M}{M_*^{n+2}} \frac{H(r)}{r^{n+1}} \quad (\text{2.29 revisited})$$

the horizon equation  $V(r) = 1$  is fulfilled at  $r = r_H$ . The physical meaning of  $M$  is the mass of a Black Hole of radius  $r_H$  [57]. When substituting  $n+1$  powers of  $M_*$  by  $M_* = 1/L_*$ , one can easily relate

$$M = (n+2) \left( \frac{r_H}{L_*} \right)^{n+1} \frac{1}{H(r_H)} M_*. \quad (3.3)$$

### 3.2 Horizons

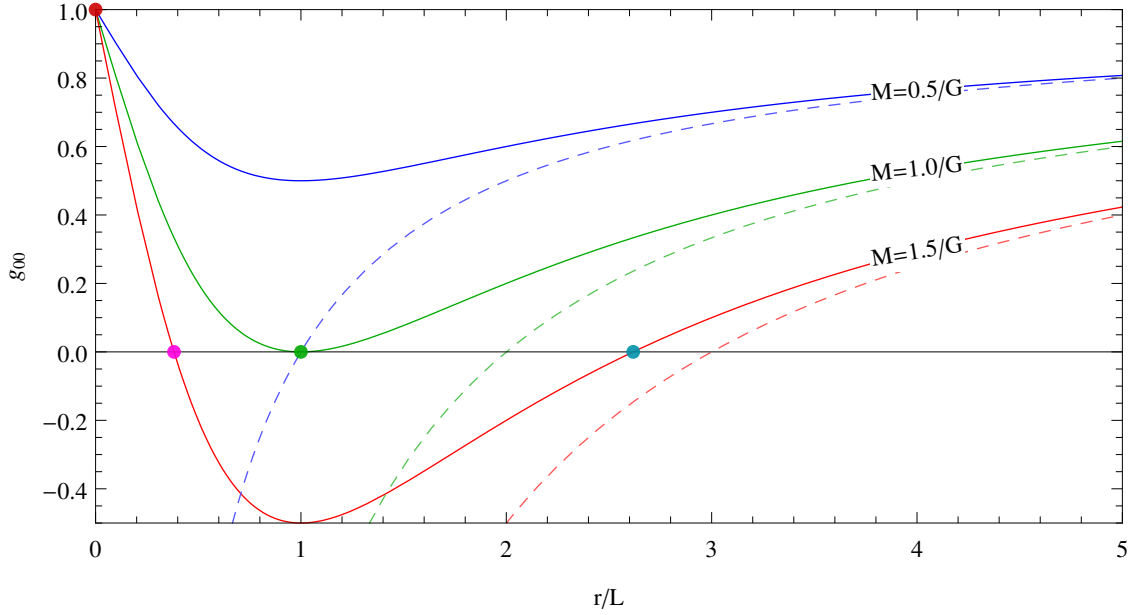
The event horizon equation, considering  $r_H$  being the event horizon, requires  $0 = g_{00}(r_H)$ . For the choices of  $H(r)$ , the horizons  $r_H$  are given by the roots of the polynomials

$$0 = z^{2+n} - zm_n + 1 \quad \text{for } h(r) \quad (3.4a)$$

$$0 = z^2(z^\alpha + 1/2)^{(3+n)/\alpha} - m_n \quad \text{for } h_\alpha(r), \quad (3.4b)$$

with  $m_n = 1/(n+2)M/M_*^{n+2}$  and  $z = r/L$ . The number of (physically meaningful) solutions depends on  $m_n$ , that is, on the Black Hole mass  $M$ . For any  $n$ , there are three possible solutions, plotted in figure 3.1:

(a)  $g_{00}$  for the holographic metric ( $h$ ).



(b)  $g_{00}$  for the self-regular metric ( $h_\alpha$ ) with  $\alpha = \alpha_0$ .

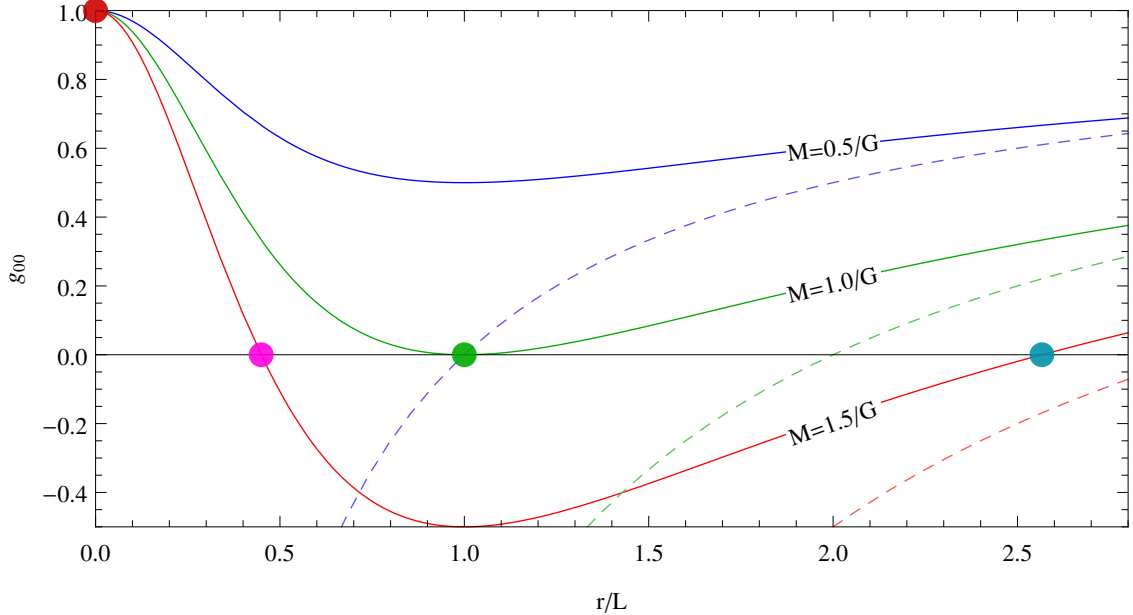


Figure 3.1: The remnant picture for  $n = 0$ . The three curves represent a smaller than critical-mass (blue), critical mass (green) and a too heavy mass (red). In any case the dashed line corresponds to the equivalent Schwarzschild metric. Note the different behaviour as  $z = r/L \rightarrow 0$ .

The colors of the dots indicate the associated radii in the penrose diagrams in figure 3.6.

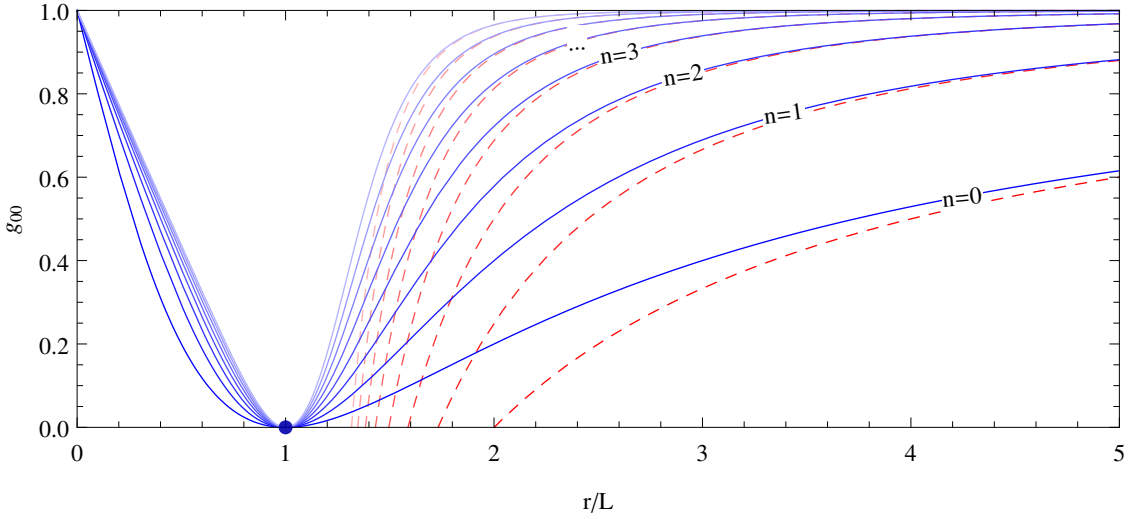


Figure 3.2: The holographic metric in the extra dimension scenario, compared with the Schwarzschild-Tangherlini metric (dashed line), for the self-encoding masses  $M_*$ . All curves are scaled for the individual  $L_*$  according to the numerical values given in table 3.1.

Compared to the fourdimensional metric (fig. 3.1a), one can see that the picture basically *stays the same*. In this figure, the curves qualitatively get “sharper” with increasing  $n$ , which corresponds to the increasing surface to volume ratio of  $n$ -spheres, which is a purely geometrical effect.

$M < M_*$  The mass is too small to create a Black Hole. In the case of the self-regular metric, the physical object is called a *G-lump* after Dymnikova [22] and represents a vacuum, self-gravitating, regular, particle-like structure [1].

$M > M_*$  There are two horizons with radii  $r_\pm$ . In figure 3.1, they are indicated by red dots. Physically, one can argue that the outer horizon  $r_+$  is the more relevant one, since it *shields* the Black Hole inner structure. Mathematically,  $r_-$  is a cauchy horizon, and in the region  $r_- < r < r_+$ , where  $g_{00} < 0$  and  $g_{rr} > 0$ , the coordinates  $r$  and  $t$  switch their meaning (cf. section 3.5).

There are no meaningful compact analytic expressions for the values of  $r_\pm$ , except for the holographic metric and without extra dimensions ( $n = 0$ ), as already given in [56]:

$$r_\pm = GM \pm \sqrt{G^2 M^2 - 4}. \quad (3.5)$$

For  $n > 0$  and especially for the self-regular metric, the roots of (3.4) can simply be determined numerically.

Note that for  $M \gg M_*$ ,  $r_+$  approaches the Schwarzschild-Tangherlini horizon.

$M = M_*$  The two horizons merge to a single horizon which are called  $r_\pm = r_0$ . This is the *extremal* radius, identified with the extremal mass  $M_*$ . In figure 3.1, the green line displays the gravitational potential with extremal mass, showing a single horizon, indicated by the green dot.

### 3.3 The self-encoding remnant

The extremal Black Hole configuration  $M = M_*$  is a feature of the nonlocal matter density. This configuration has special thermodynamical properties which will be discussed in the next chapter. First, the situation of length scales of our models  $H(r)$  is clarified. One finds the extremal radius  $r_0$  with the remnant equations:

$$\begin{cases} \partial_r|_{r=r_0} g_{00}(r) = 0 \\ g_{00}(r_0) = 0 \end{cases} \quad (3.6)$$

$n$	0	1	2	3	4	5	6	7
$h$	$L_*$	1.00	0.79	0.76	0.76	0.76	0.77	0.78
	$M_*$	1.00	1.26	1.32	1.32	1.31	1.29	1.28
	$G_*$	1.00	1.59	1.73	1.74	1.71	1.67	1.63
$h_\alpha$	$\alpha_0$	1.755	4.285	7.081	9.333	10.642	11.128	11.098
	$L_*$	1.	0.851	0.856	0.862	0.86	0.851	0.839
	$M_*$	1.	1.176	1.168	1.16	1.163	1.175	1.192
	$G_*$	1.	0.724	0.733	0.743	0.739	0.725	0.704

Table 3.1: Numerical results for equations (3.8): The self-encoding horizon radius  $r_0 = L_*$ , remnant masses  $M_* = 1/L_*$  and reduced coupling (Newtons) constant  $G_* = M_*^2$ . These numbers are given in multiples of  $L_P = \sqrt{\hbar G/c^3} \approx 10^{-35}$  m, the 4d Planck unit. For the self-encoding model, all values are given for  $\alpha = \alpha_0$  (also displayed), as derived in equation (3.13).

For the generic potential (2.29), one can we rewrite the first equation to

$$\partial_r V(r)|_{r=r_0} = 0 = -(n+1) \frac{H + (r_0)}{r_0} + H'(r_0) = L H'(z_0) - \frac{n+1}{z} H(z_0) \quad (3.7)$$

This equation can be solved for both  $h(r_0)$  and  $h_\alpha(r_0)$ . This yields

$$r_0 = \tilde{r}_0 \left( \frac{1}{1+n} \right)^{\frac{1}{2+n}} \quad \text{and} \quad r_{0,\alpha} = \tilde{r}_0 \left( \frac{1}{1+n} \right)^{\frac{1}{\alpha}}. \quad (3.8a, 3.8b)$$

Equation (3.8) allows to connect the length scale  $\tilde{r}_0$  introduced for the holographic and self-regular model to a physical length scale  $r_0$ . Note that the *self-encoding* principle requires that the size of the remnant  $r_0$  should be identical to the fundamental length scale of the physical theory  $l_0$ . For gravity in 4d space time, the only fundamental length scale is given by the coupling constant (Newtons constant)  $G$  which defines the Planck length  $L_{\text{Pl}} = \sqrt{G} \approx 10^{-35}$  m. In 4d, (3.8) assures this is true, as already stated in [56]:

$$r_0 \stackrel{!}{=} l_0 = L_{\text{Pl}} = \tilde{r}_0. \quad (3.9)$$

With extra dimensions, there is the reduced Planck length  $L_*$  which is the actual fundamental length scale  $l_0$ , since the observable Planck length  $L_{\text{Pl}}$  is just an effective one. To express  $h(r)$  and  $h_\alpha(r)$  only in terms of  $L_*$ , require  $r_0 \stackrel{!}{=} l_0 = L_*$  and find

$$\tilde{r}_0 = (1+n)^{\frac{1}{2+n}} L_* \quad \text{and accordingly} \quad \tilde{r}_0 = (1+n)^{\frac{1}{\alpha}} L_*. \quad (3.10a, 3.10b)$$

When computing  $M(r_0)$ , the self-encoding of the fundamental mass scale  $M_*$  is expected, that is,  $M(r_0) = M_*$ . For the holographic metric, it is  $h(L_*) = 1/(2+n)$  and thus

$$M(L_*) = \frac{1}{n+2} \left( \frac{L_*}{L_*} \right)^{1+n} \frac{1}{h(L_*)} M_* = M_*. \quad (3.11)$$

In case of the self-regular metric,  $\alpha$  must be fixed to ensure  $M(r_0) = M_*$ . Using the mass (3.3), it reads

$$M(r_H) = \underbrace{\frac{1}{n+2} \left( \frac{3+n}{2} \right)^{\frac{3+n}{\alpha}} \left( \frac{r_0}{L_*} \right)^{n+1}}_{\stackrel{!}{=} 1} M_* = M_* \quad \text{with } \alpha = \alpha_0 \quad (3.12)$$

This gives us the self-encoding value for the  $\alpha$  parameter:

$$\alpha_0 = \frac{3+n}{\ln(2+n)} \ln \frac{3+n}{2}. \quad (3.13)$$

### 3.4 The regular core

As announced in section 2.6, the self-regular metric offers a non-diverging curvature at the origin. The Ricci scalar is according to (2.21) given by

$$R(r) = R_N^N = \frac{(n+2)V(r)}{r^2} + V''(r) \quad (3.14a)$$

$$= \frac{2}{2+n} \frac{M}{M_*^{2+n}} \frac{(2+n)^2 H(r) - 2(1+n)rH'(r) + r^2 H''(r)}{r^{3+n}} \quad (3.14b)$$

One can give an estimation for  $R(0)$  based on the taylor expansions of  $H(r)$  at  $r = 0$ :

$$3h(r) = (r/L)^{2+n} + \mathcal{O}\left((r/L)^{2(2+n)}\right), h'(r) \approx (r/L)^{1+n}, h''(r) \approx (r/L)^n \quad (3.15)$$

$$h_\alpha(r) = (r/L)^{3+n} + \mathcal{O}\left((r/L)^{2(3+n)}\right), h'_\alpha(r) \approx (r/L)^{2+n}, h''_\alpha(r) \approx (r/L)^{1+n} \quad (3.16)$$

Inserting this into  $R(r)$  for  $H(r)$ , equation (3.14b), gives  $H(0) \approx L/r$  for the holographic metric whereas the self-regular metric exposes a finite value at  $R(0)$  as soon as  $\alpha > 0$ , c.f. figure 3.3. This is the reason for the naming of the self-regular metric.

Actually there are reviews about the quite general family of regular Black Holes, e.g. by Ansoldi [1] or Hayward [32]. As can be seen in the next section 3.5 about their conformal picture, regular Black Holes enjoy special properties.

To learn more about the origin of the regularity, one can investigate the limit  $\alpha \rightarrow \infty$ , plotted in figure 3.4. At  $\alpha \rightarrow \infty$ , the two phases of the Black Hole clearly stand out. For simplicity, one should discuss the case in  $n = 0$  and  $M = M_*$ . It is

$$\lim_{\alpha \rightarrow \infty} g_{00} = \begin{cases} 1 - 2GMr^2 & , r < L \\ 1 - \frac{2GM}{r} & , r > L. \end{cases} \quad (3.17)$$

Recognize the de Sitter space gravitational potential from section 1.2.3,

$$g_{00} = 1 - \frac{\Lambda}{3}r^2, \quad (\text{1.23 revisited})$$

with positive cosmological constant  $\Lambda = 2/3GM$  and positive constant curvature  $R = 4$  (cf. figure 3.3). This is called the de Sitter *core* since for physical meaningful theories,  $r < \infty$ .

What is the meaning of the cosmological vacuum solution like de Sitter in the context of Quantum Black Holes? EFE relate space-time  $G_{\mu\nu}$  to matter density  $T_{\mu\nu}$ . In this thesis, the term *dual theory* will be frequently encountered, which means shifting contributions between  $G_{\mu\nu}$  and  $T_{\mu\nu}$ . In this context, the dual theory to de Sitter space-time as a solution of EFEs with cosmological constant and zero energy momentum tensor  $T_{\mu\nu}$  is EFE without cosmological constant but shifted contributions inside the energy momentum tensor. This idea goes back to Dymnikova [22], but is also already discussed in text books as vacuum polarisation [46, p. 411]. In the quantum picture, this is interpreted as the *Quantum Vacuum* and is characterized by its *outward pressure* we were encountered with already at the time of the derivation of the Black Hole, equation (2.19) that defines the tangential pressure as

$$p = \rho + \frac{r}{n+2} \partial_r \rho > 0. \quad (3.18)$$

One can imagine this type of pressure as the one driving a fermi gas and refer to it as degeneracy pressure. This kind of pressure also prevents the G-lump from collapsing in its own gravitational inward pressure.

For a review about regular interiors of Schwarzschild-like Black Holes with  $T_0^0 = T_1^1$ , see also [23].

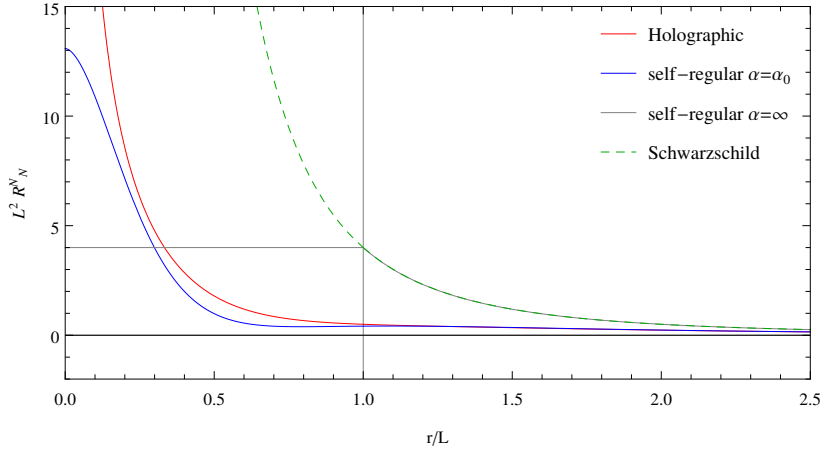


Figure 3.3: The curvature scalar  $R$  for  $n = 0$ ,  $GM = 1$ ,  $\alpha = 3\alpha_0$  holographic (red) and self-regular model (blue). While the curvature diverges for the holographic Black Hole, any value of the self-regular Black Hole achieves a finite value  $R(0)$ .

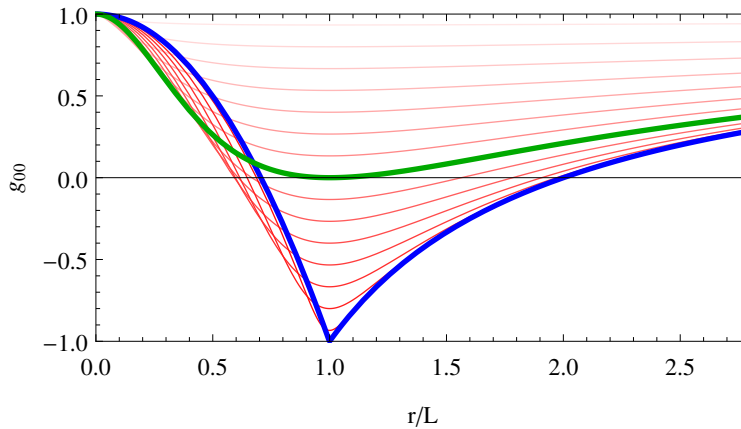


Figure 3.4: Self-regular:  $g_{00}$  for  $M = 1$  and different choices of  $\alpha \in \{0, 20\}$ . The blue curve shows the limit  $\alpha \rightarrow \infty$  where the behaviour is clearly separated: For  $r < L$  there is a de Sitter metric, beyond  $r > L$  there is a Schwarzschild metric. Color saturation encodes the  $\alpha$  scale. The special self-encoding choice  $\alpha = \alpha_0$  is highlighted as green line, corresponding to figure 3.1b.

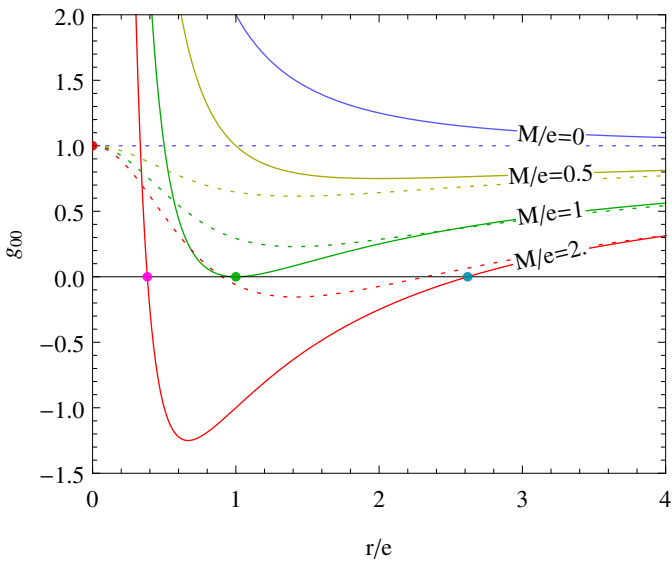


Figure 3.5: The Reissner-Nordström gravitational potential for different mass-charge ratios  $M/e$ , compared with the Bardeen solution for the same mass-charge ratios (dashed lines).

### 3.5 Conformal Structure

It is often helpful to transform coordinates in a way that the global structure of space-time is mapped on a finite diagram. If this mapping is conformal (preserving angles locally) and two-dimensional, such diagrams are called (*Carter-Penrose*) *Penrose diagrams*. Penrose diagrams are subject to any GR textbook that deals with Black Holes, e.g [31, 46, 75].

The three Penrose diagrams that represent the three possible space-times presented in section 3.2 are displayed in figure 3.6. It is the diagram of a *regular Black Hole* which resembles the structure of the *Reissner Nordström* (RN) Black Hole which describes static nonrotating Black Holes with electrical charge  $e$  in  $d = 4$  (with  $G = 4\pi\epsilon_0 = c = 1$ ),

$$V(r) = \frac{2M}{r} - \frac{e^2}{r^2} = 2\frac{M}{e} \frac{z-1}{z^2} \quad \text{with } z = r/e, \quad (3.19)$$

but singularity-free in the case of the regular Black Hole. This similarity dates back to the regular Black Hole by Bardeen (reviewd e.g in [1]), given by the gravitational potential

$$V(r) = \frac{2Mr^2}{(r^2 + e^2)^{3/2}} = 2\frac{M}{e} \frac{1}{(1 + e^2/r^2)^{3/2}}. \quad (3.20)$$

The Bardeen metric a special case of the self-regular Black Hole with parameters  $\alpha = 2$ ,  $\tilde{r}_0 = 2^{1/\alpha}e$  and is compared to the RN Black Hole in figure 3.5. In this figure, one sees that the hyper-extreme case  $M < e$  is replaced by G-lumps, giving flat space for  $M/e \rightarrow 0$ . This cures both the naked singularity as well as the repulsive gravity regime ( $g_{00} > 1$ ).

One can discuss the penrose diagrams shortly without going into detail how to find the maximally extended space-time that describes space-time everywhere, taking up the distinction of cases in section 3.2. Figure 3.6 contains three panels:

- (a) The G-lump is probably the biggest achievement for the charged Black Hole, as it cures the naked singularity, while it is not the object of interest in this context.
- (b) The conformal diagram for the maximally extended Black Hole is periodic on the vertical axis on infinite extend (“isometric” regions). There are three classes of regions: the untrapped and asymptotically flat space time region **I**. The timelike region of trapped surfaces **II**, characterized by  $r_- < r < r_+$ , connects outer **I** and core **III** regions. The again space-like and untrapped region **III** is hyperbolic, as dominated by de Sitter behaviour. Note that in this space-time, it is possible to *wrap around the universe* by starting from **I**, travelling **II** and **III** and leaving the Black Hole near zone again over **II** to **I**, all inside a causal light-cone with  $45^\circ$  angles.
- (c) The extremal situation also made the singularity accessible from outside by travelling from region **I** to **III**. This is cured with a regular origin.

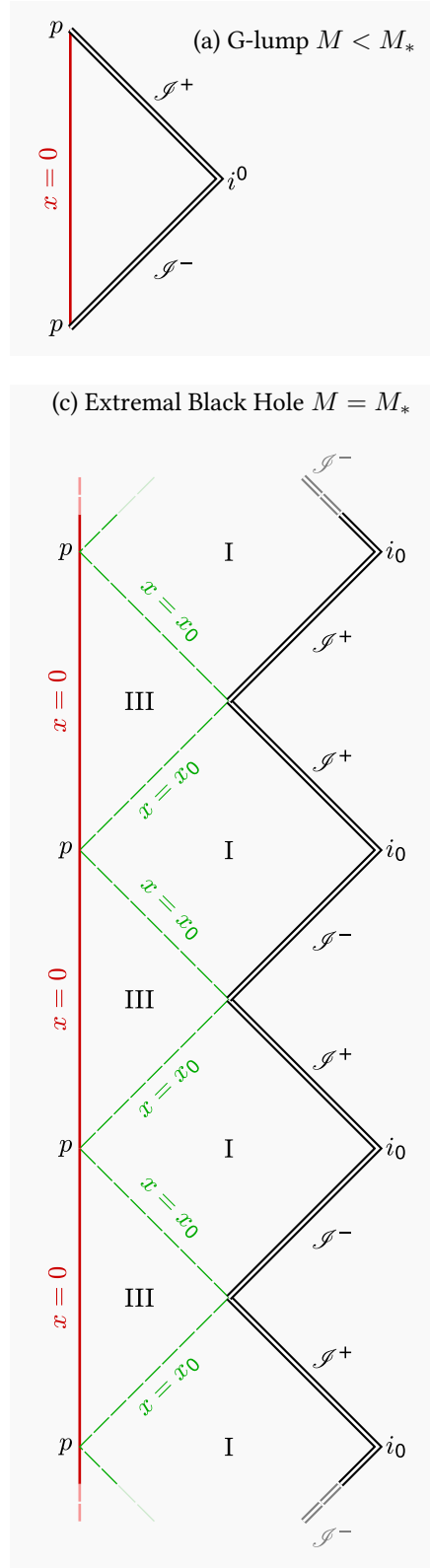
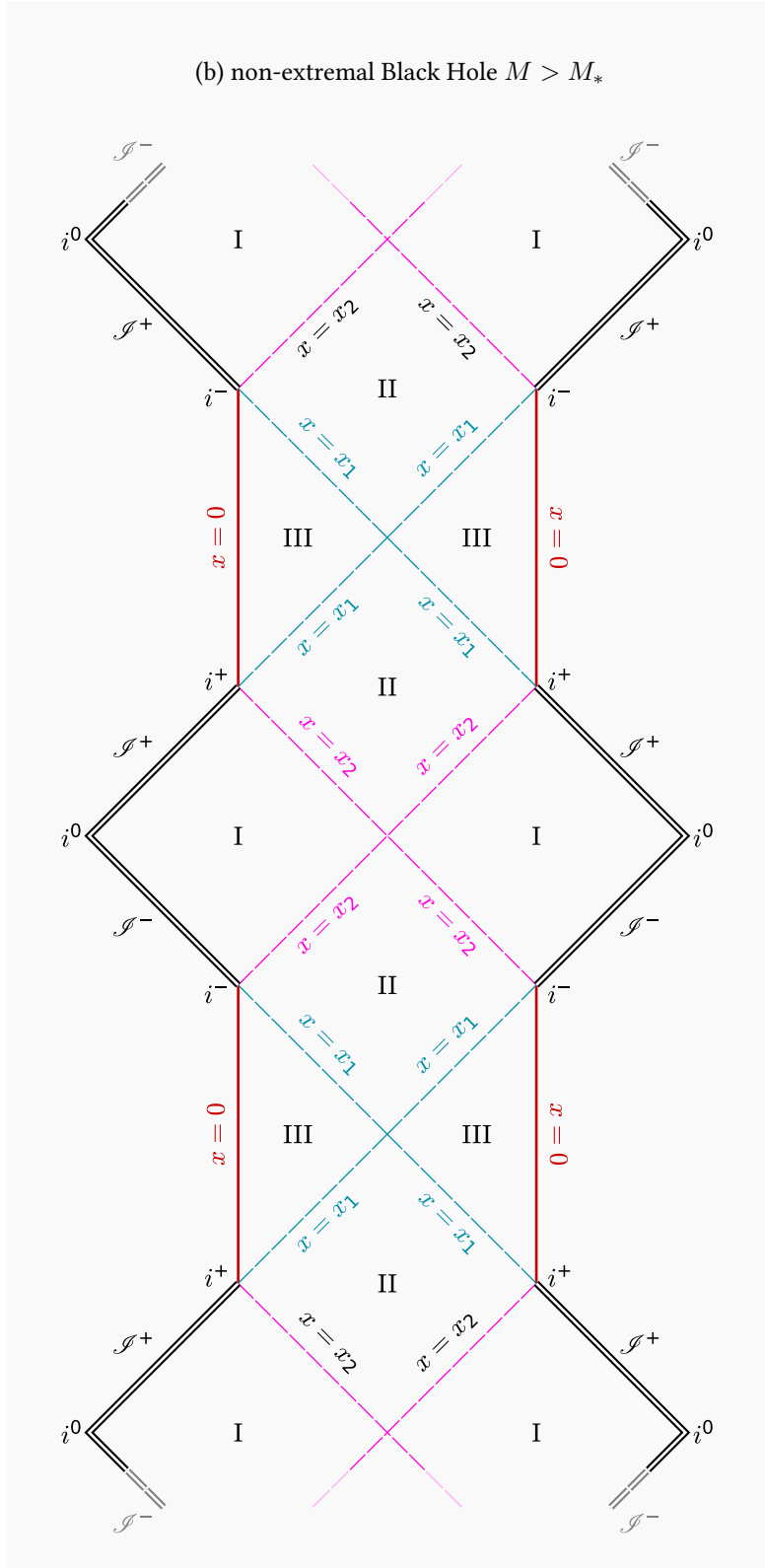


Figure 3.6: The penrose diagrams of the regular Black Holes, after [1, 32, 49].  $x$  is a dimensionless coordinate  $x = r/e$  and  $x_2 = r_+/e$  is the outer horizon, while  $x_1 = r_-/e$  is the inner horizon.  $x_0 = r_0/e$  is the extremal horizon. The colors of constant horizons  $x$  in these diagrams match the colors of the according coordinates in figure 3.1 and 3.5. This diagram is basically the same for both Reissner Nordström and the holographic metric, where there are singularities at  $x = 0$ .

## 3.6 Energy conditions

Energy conditions in General Relativity are a tool to put constraints on matter distributions (that is, energy-momentum tensors) in a way how some expects them to behave. They are formulated from a classical viewpoint and not deduced from Einstein field equations or other first principles. Roughly speaking, they generalize the statement that one does not observe negative masses or regions of negative mass distribution.

Approaches to quantum gravity regularly violate energy conditions, and by examining how and where they violate these conditions, one understands about the quantum nature in General Relativity. For example, one expects energy conditions in delta smearing densities to be local around the Black Hole, e.g. violations occur in a region  $r \lesssim L_*$  while they hold for  $r \gtrsim L_*$ . As Ansoldi notes, this is cannot be taken for granted in a non linear theory as General Relativity is [1].

We check the following energy conditions (EC):

- **Null EC**, defined that for every (future) *null* vectors  $x^\mu$  the observed matter density

$$\rho_{\text{obs}} = T_{AB}x^A x^B \quad (3.21)$$

is non negative,  $\rho_{\text{obs}} \geq 0$ . In words, this means a matter density  $\rho_{\text{obs}}$  observed by a *light ray* must be positive. A null vector fulfills  $x_A x^A = -x_0^2 + x_1^2 + \sum_{i=2}^{3+n} x_i^2 = 0$ , and if it is a *future* null vector,  $x_A > 0 \forall A$ . Since  $T_{AB} \sim \text{diag}(-\rho, -\rho, p, \dots, p)$  we get

$$\rho_{\text{obs}} \sim -\rho x_1^2 + \sum_{i=2}^{3+n} p x_i^2 = -\rho x_1^2 + p(x_0^2 - x_1^2) = -(\rho + p)x_1^2 + px_0^2 \stackrel{!}{\geq} 0 \quad (3.22)$$

The negative contribution is governed by

$$f_{\text{weak}}(r) := \rho + p = 2\rho + \frac{r}{n+2} \partial_r \rho. \quad (3.23)$$

In regions where  $f_{\text{weak}}(r) > 0$ , it is violated.

- **Strong EC** requires basically the same for any (future) *timelike* vector  $x^\mu$ . We find it violated when

$$f_{\text{strong}}(r) = (2+n)p. \quad (3.24)$$

- **Dominant EC** requires for any (future pointing) timelike or null vector  $x^\mu$  that  $-T_B^A x^B = -T_A^A x^A = y_A$  is a future timelike or null vector.

- **Weak EC** is proven by [1] that it is always fulfilled.

To do: Plot energy conditions of my BHs. One will see that the only violated energy condition is the strong energy condition in the regime  $r < L_*$ . This is an indicator that we are dealing with quantum matter that does not behave classically. A positive result is that the quantum character of the matter densities is localized around the origin, so far distance classical behaviour is ensured.

# Chapter 4

## Thermodynamical properties

This chapter is dedicated the derivation and discussion of the temperature, stability and entropy of the Black Hole remnant. This means the non-extremal Black Hole configurations are no more discussed here.

Law	Thermodynamics	Black Holes
0.	$T$ constant on a body in thermal equilibrium	$\kappa$ constant on horizon of (stationary) BH
1.	$dE = TdS - pdV + \mu dN$	$dM = \frac{\kappa}{8\pi}dA + \Omega_H dJ + \Phi dq$
2.	$\delta S \geq 0$	$\delta A \geq 0$
3.	$T = 0$ cannot be reached	$\kappa = 0$ cannot be reached

Table 4.1: The laws of thermodynamics correspond with Black Hole thermodynamics

### 4.1 Hawking Temperature

The Hawking temperature  $T_H = \kappa/4\pi$  is defined by means of the surface gravity  $\kappa = \partial_r g_{00}|_{r=r_H}$ . Here, one can insert  $r_H = r_0$  and get for generic  $H(r)$  the temperature

$$T_H = \frac{1}{4\pi} \left( \frac{1+n}{r_H} - \frac{H'(r_H)}{H(r_H)} \right). \quad (4.1)$$

Taking the Schwarzschild limit according to section 2.6.3, let  $H'/H \rightarrow 0$  and eventually get the well known 4d Schwarzschild temperature  $T = 1/(4\pi r_H)$ . The  $H'/H$  term is the quantum correction.

It is simple to insert the  $\{h, h_\alpha\} \in H$ , figure 4.1 shows  $T_H$  for both of them. For the sake of completeness,  $T_H$  is given for both models here explicitly:

$$T_H = \frac{1}{4\pi r_H} \left( 1 + n - (2+n) \frac{(L/r)^{(2+n)}}{1 + (L/r)^{(2+n)}} \right) \quad \text{for } h(r) \quad (4.2)$$

$$T_H = \frac{1}{4\pi r_H} \left( 1 + n - \frac{(L/r)^{4+n}}{1 + \frac{1}{\alpha}(L/r)^{3+n}} \right) \quad \text{for } h_\alpha(r) \quad (4.3)$$

Below  $r \lesssim 3L_p$ , the temperature differs significantly from the Schwarzschild temperature. There is a maximum temperature at a critical radius  $r_C$  (indicated by the dots in fig. 4.1, numerical values are given in table 4.2), and for smaller radius the Black Hole cools down until it reaches zero temperature at  $r_0$ . One therefore speaks of a *cold* remnant.

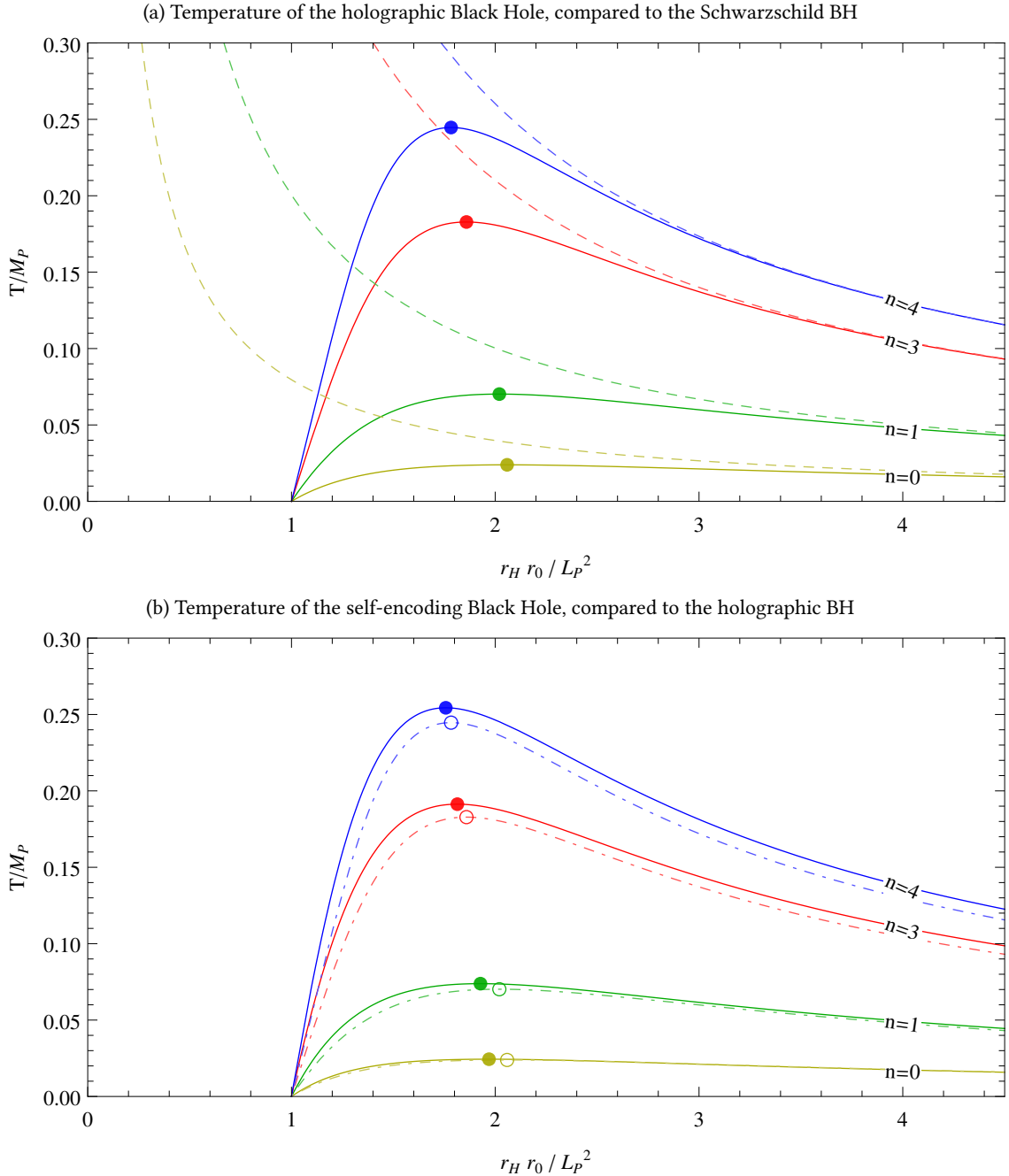


Figure 4.1: Temperature of the Black Holes for different extra dimensions  $n$ . While the x-axis scaling depends on  $n$  ( $r_0$  given in equation 3.8a), the y-axis is scaled by  $M_{\text{Pl}}$  in 4 dimensions, to show the increasing heat. The circles indicate the critical radii.

In frame (a), the dashed lines corresponds to the classical Hawking-Beckenstein temperature of the Schwarzschild-Tangherlini metric in  $n$  extra dimensions. In frame (b), the dot-dashed line indicates the corresponding temperatures of the holographic metric.

$n$	0	1	2	3	4	5	6	7
$r_C$	2.060	1.600	1.480	1.410	1.360	1.330	1.300	1.280
$r_{C,\alpha_0}$	1.970	1.460	1.340	1.290	1.260	1.250	1.230	1.220
$T(r_C)$	0.024	0.070	0.124	0.183	0.245	0.309	0.375	0.443
$T(r_{C,\alpha_0})$	0.024	0.074	0.131	0.191	0.254	0.319	0.386	0.454

Table 4.2: Critical radii  $r_C$  for different dimensions, for the holographic ( $r_C$ ) and self-regular ( $r_{C,\alpha_0}$ , so  $\alpha = \alpha_0$ ) Black Holes, and maximum temperatures of the according Black Holes. All values are given in 4d Planck units.

## 4.2 Heat capacity

The heat capacity is an extensiv thermodynamical property, defined as measure of the heat added to an object resulting from a temperature change, in terms

$$C = \frac{Q}{\Delta T}. \quad (4.4)$$

For Black Hole thermodynamics, one can identify  $Q = M$  and use the Hawking temperature just derived to compute the heat capacity. Since it is virtually not possible to exress  $M = M(T_H)$ , insert  $1 = \partial r_H / \partial T_H$  and compute

$$C = \frac{\partial M}{\partial T_H} = \frac{\partial M}{\partial r_H} \left( \frac{\partial T_H}{\partial r_H} \right)^{-1} = \frac{\partial M}{\partial z_H} \left( \frac{\partial T_H}{\partial z_H} \right)^{-1}. \quad (4.5)$$

For generic  $H(r)$ , inserting temperature (4.1) and mass (3.3), one can do the elaborate computation and ends up with the compact expression

$$C = -\frac{4\pi r_H^{n+2}}{M_*^{n+2}} \frac{(n+1)H(r_H) - r_H H'(r_H)}{r_H^2 H(r_H) H''(r_H) - r_H^2 H'(r_H)^2 + (n+1)H(r_H)^2} \quad (4.6)$$

Now inserting choices for  $H(r)$  is quickly done. Figure 4.2 shows the graph of  $C$  for the holographic and self-encoding metric.

By simply letting  $H, H', H'' \rightarrow 0$  according to section 2.6.3, one ends up with the diverging heat capacity of ordinary Schwarzschild Black Hole:

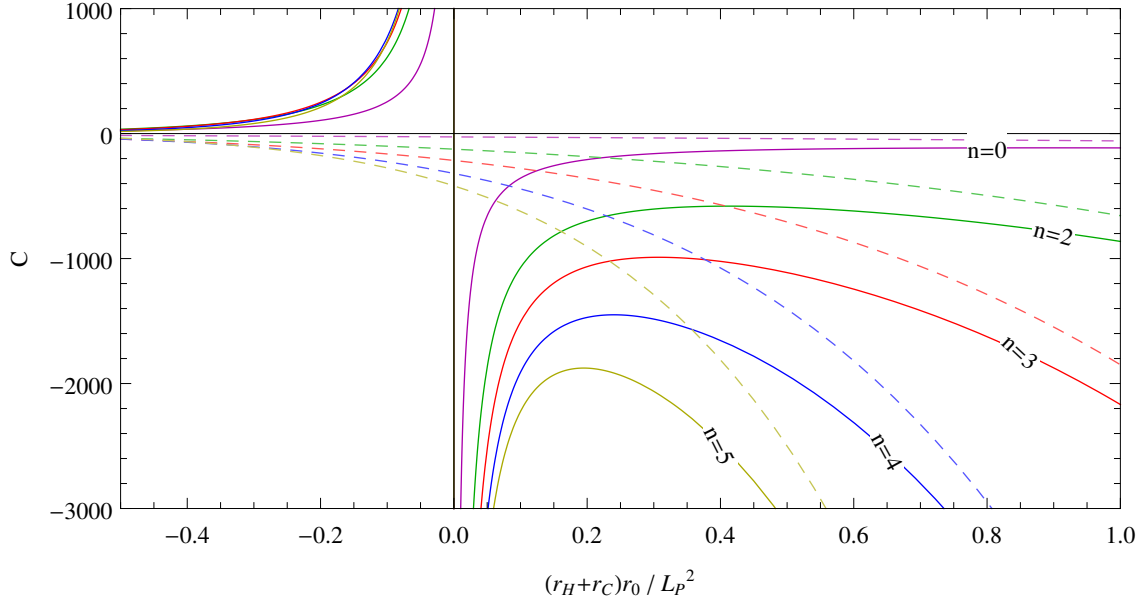
$$\begin{array}{ccc} C & \xrightarrow{H \rightarrow \delta} & -4(1+n)\pi r_H^{2+n}/M_*^{2+n} \\ n \rightarrow 0 \downarrow & & \downarrow n \rightarrow 0 \\ -4\pi r_H^2 G \frac{H-r_H H'}{r_H^2 H H'' - r_H^2 H'^2 + H^2} & \xrightarrow{H \rightarrow \delta} & -4\pi r_H^{2+n} G \end{array} \quad (4.7)$$

In contrast to the Schwarzschild solution, for the choice of smeared  $H(r)$ , the heat capacity undertakes two changes of sign, one of them when a phase transition takes place ( $C \rightarrow \pm\infty$ ). This is called the critical radius  $r_C$ . At this point, the Black Hole temperature  $T_H(r_C)$  (eq. 4.1) is maximal:

$$\partial_{r_H} T_H|_{r_H=r_C} = 0 \Leftrightarrow z_C = \sqrt{\frac{1+n}{H'(z_C) - H''(z_C)H(z_C)}} H(z_C). \quad (4.8)$$

The expression (4.8) suggests investigating the  $H(z) \rightarrow \Theta(z)$  limit, but of course the Schwarzschild Black Hole has no extremal temperature. Mathematically,  $z_C \rightarrow \infty$ , but there is no physical content in this result.

(a) Heat capacity of the holographic Black Hole, compared to the Schwarzschild BH



(b) Heat capacity of the self-encoding Black Hole, compared to the holographic BH

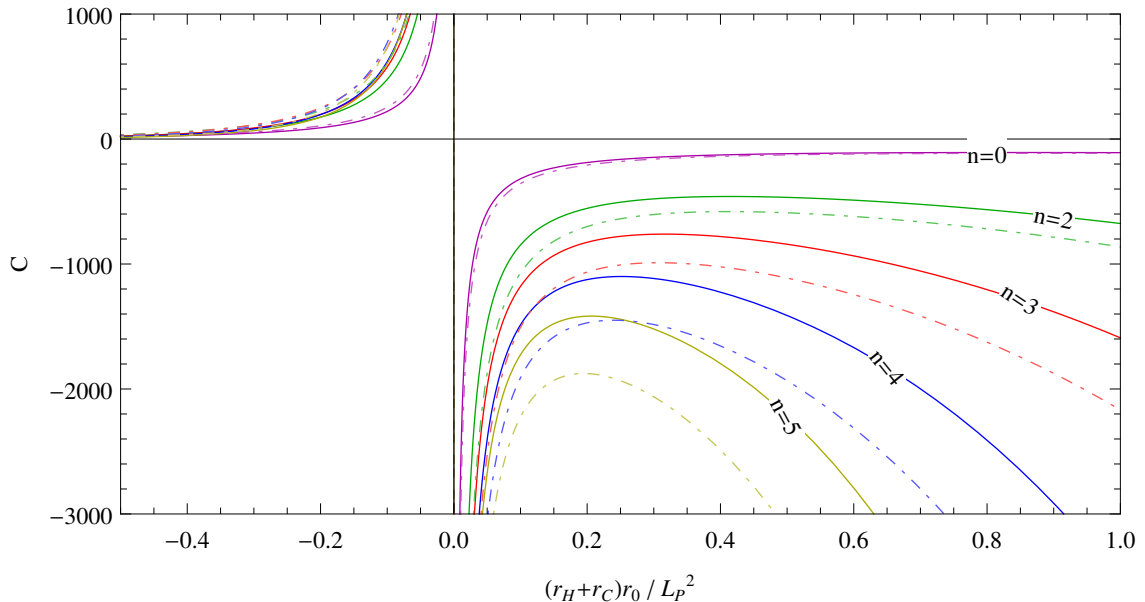


Figure 4.2: Heat capacity of Black Holes for different extra dimensions  $n$ . For each dimensions  $n$ , the x-axis is shifted to the critical radius and scaled by the horizon length  $r_0$  as given in equation 3.8a. In frame (a), the dashed lines corresponds to the heat capacity of the classical Hawking-Beckenstein Black Hole in  $n$  extra dimensions. In frame (b), the dot-dashed line corresponds to the corresponding heat capacity of the holographic metric.

The critical radius for  $h(r_C)$  and  $h_\alpha(r_{C,\alpha})$  can be determined by evaluating the extremal temperature condition (4.8):

$$r_C = 2^{\frac{1}{n+2}} \left( (2+n)\sqrt{n^2 + 2n + 5} - n^2 + 3n - 4 \right)^{-\frac{1}{n+2}} L, \quad (4.9)$$

$$r_{C,\alpha} = 2^{\frac{1}{\alpha}} \left( \sqrt{(3+n)(3+n+\alpha(2+3\alpha+(\alpha-2)n))} + (n-1) - \alpha(3+n) \right)^{-\frac{1}{\alpha}} L. \quad (4.10)$$

The critical radius was used to rescale the abscissa in figure 4.2, so  $(r_H - r_C)r_0$  is displayed. Thus it is easier to compare  $C$  for a different number of dimensions. Numerical values for  $r_C$  are given in table 4.2.

### 4.3 The Phase transition

Eventually, having computed  $g_{00}$ ,  $T$  and  $C$ , one is able to compare those quantities for Black Hole stability discussion. Figure 4.3 illustrates the curves and different phases, exemplary for the holographic Black Hole. Considering the sign of the heat capacity, three phases can be distinguished:

$r > r_c$ . The heat capacity is negative, the system is unstable: Losing mass by radiation makes it hotter and hotter. This behaviour is well described by the Schwarzschild metric.

When reaching  $r \rightarrow^+ r_c$ , in the modified metrics this process stagnates, the temperature rises no more. Now a phase transition takes place at  $r_C$ , the system gets stable.

$r_0 < r < r_C$ . The heat capacity is positive and the Black Hole system is stable. Losing mass now results in losing temperature. The system heavily deviates from the classical Schwarzschild solution. The Temperature decreases until it eventually reaches zero.

$r < r_0$ . There is an event horizon at  $r_0$  which is possibly the smalles possible event horizon, rejecting the answers for questions after physical properties beyond the reason. In this model, the heat capacity again gets negative, but in the same way the temperature gets negative, giving rise to its physical interpretation.

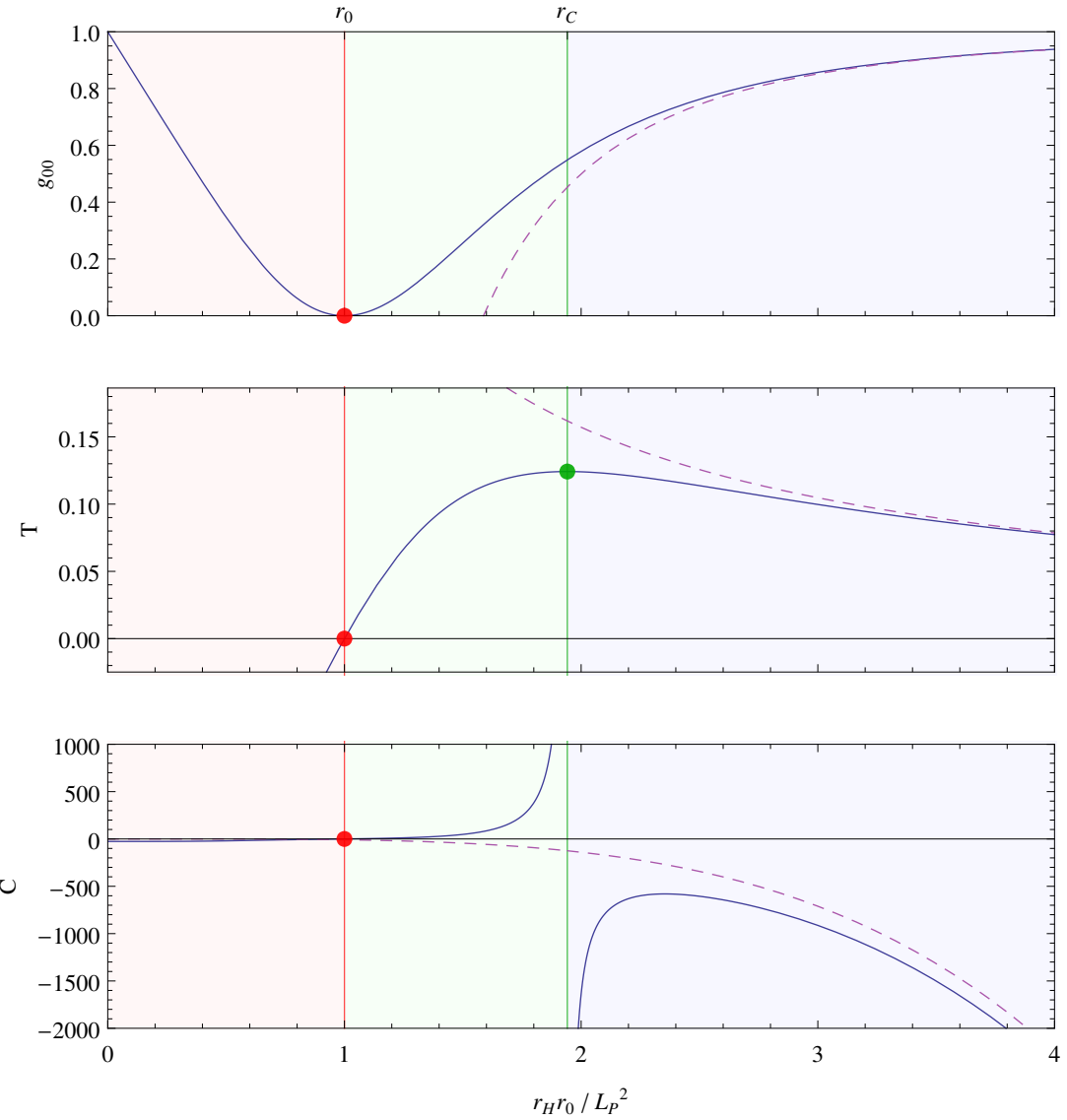


Figure 4.3: Comparison of first metric coefficient ( $g_{00}$ , top panel), temperature (middle panel) and heat capacity (bottom panel) on the same scale. The blue curve represents the holographic Black Hole for an arbitrary dimension (here:  $n = 2$ ). The dashed curve is the corresponding Schwarzschild behaviour. Regarding the sign of the heat capacity (Sign  $C = \pm 1$ ), there are three different states, indicated by colors and separated by  $r_0$  (red line) and  $r_C$  (green line).

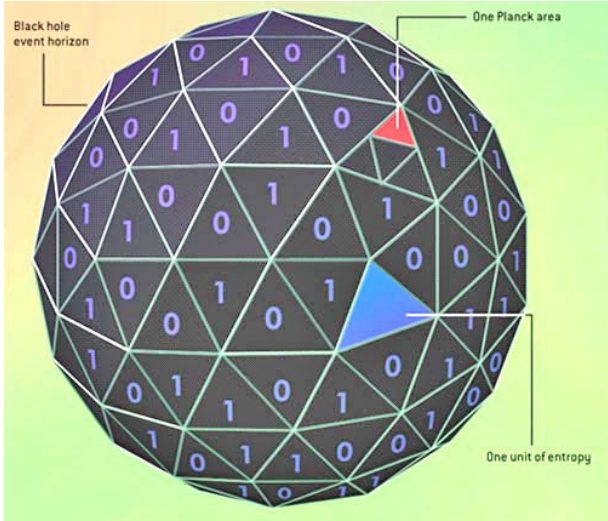


Figure 4.4: An artistic interpretation of the holographic principle, as it illustrated an science magazine article by Jacob Bekenstein [7]. The Black Hole entropy is quantized in terms of Planck units. A Planck area (blue) has  $A/4$  units of entropy (red).

## 4.4 Entropy

Entropy as a measure for micro states in a thermodynamical system is in the context of Black holes thermodynamics maybe the most interesting quantity. The entropy is defined as

$$S = \int \frac{dM}{T}. \quad (4.11)$$

The entropy defining integral can also be substituted like in the heat capacity in the section before, giving for generic  $H$  a compact expression:

$$S(r) = \int \frac{dM}{T} = \int dr_H \left( \frac{1}{T} \frac{dM}{dr_H} \right) = 4\pi m_n \int dr_H \frac{r_H^{1+n}}{H(r_H)} \quad (4.12)$$

Approaching the limit  $H \rightarrow \Theta$ , one gets the Schwarzschild entropy curve

$$4\pi m_n \int dr_H r_H^{1+n} = \frac{4\pi m_n}{1+n} r_H^{2+n} \xrightarrow{n \rightarrow 0} 8\pi G r_H^2 \quad (4.13)$$

Compared to that curve, for the holographic model in  $n$  dimensions the entropy integral (4.12) has the value

$$S_h(r) = 4\pi m_n \left( \frac{r^{n+2}}{n+2} + \log(r) \right). \quad (4.14)$$

Note the *logarithmic quantum corrections*. They motivate the label *holographic* for the  $h(r)$ -smeared metric. If the metric would not scale for higher dimensions, the entropy (for  $h(r) = 1/(1 + (L/r)^2)$  in any  $n$ ) would look like

$$S = 4\pi m_n \left( \frac{r^{n+2}}{n+2} + \frac{r^n}{n} \right) \quad \text{for } n > 0. \quad (4.15)$$

The self-encoding metric also does not possess a logarithmic entropy correction, but a hypergeometrical one:

$$S = \frac{4\pi m_n}{n+2} \left( r^2 + {}_2F_1 \left( -\frac{2+n}{\alpha}, -\frac{3+n}{\alpha}, 1 - \frac{2+n}{\alpha}; -\frac{1}{2r^\alpha} \right) \right) \quad (4.16)$$

### 4.4.1 The area quantization picture

The Black Hole area theorem dates back to Wheeler 1973 and is a recasting of the Schwarzschild Black Hole entropy in terms of the horizon area  $A = 4\pi r_H^2$ , and therewith

$$S = 2\pi \frac{A}{A_0} \quad \text{with } A_0 = 4\pi L_P^2. \quad (4.17)$$

In the same spirit, we can recast the holographic metric Black Hole (4.14) as

$$S_h(A_+) = \frac{\pi}{A_0}(A_+ - A_0) + \pi \log(A_+/A_0), \quad (4.18)$$

with  $A_+ = \Omega_{n+2} r_+^{2+n}$  and  $A_0 = \Omega_{n+2} L_*^{2+n}$ .

By means of a taylor expansion  $\log(x) \approx (x-1) + \mathcal{O}((x-1)^2)$  around  $x=1$ , one sees the entropy vanishes for  $A_+ \rightarrow A_0$ , which encodes the physical fact that the Planck size remnant can be only realized in one configuration [56]. We therefore interpret it as an *ground state* for a quantized area spectrum

$$A_+ = A_{n-1} = nA_0 = 4\pi n L_*^2, \quad (4.19)$$

to express  $A_+$  (literally) stores  $n$  basic units of information. Wheeler created a new term for this concept of *bits* and *bytes*: One byte consists of  $4\pi$  bits. This is also shown in figure 4.4.

The area quantization also motivates to a discrete mass spectrum and the analysis of a transition from a (semi-)classical regime to a quantum regime with different kinds of decay: thermal decay vs. quantum decay with discrete quanta emission. The higher dimensional extension does not change the picture drawn in [56].

The area quantization concept was also studied by Dvali [20, 21].

# Chapter 5

## Modified field equations

In this section I want to build modified Einstein field equations by recasting the modified matter term. This is done with a bilocal operator  $\mathcal{A}^{-2}$ . Considering a Schwarzschild-like matter density  $T_{\mu\nu} \sim \delta(r)$ , the  $H(r)$  smearing introduced in section 2.5.2 shall be communicated by  $\mathcal{T}_{\mu\nu} \sim \mathcal{A}^{-2}\delta(r)$ . We might write the Einstein equations for motivational purpose such as

$$G_{\mu\nu} = \mathcal{A}^{-2}\delta. \quad (5.1)$$

By now multiplying  $\mathcal{A}^{-2}$  from the left hand side, we end up with the *dual theory*

$$\mathcal{A}^2 G_{\mu\nu} = \delta. \quad (5.2)$$

In the dual theory, the nonlocality was *shifted* to the geometrical part (the Einstein tensor) of the field equations, while the matter part remains purely classical. This theory seems more fundamental than the semiclassical matter distribution.

The operator  $\mathcal{A}^2$  mediates *nonlocal* effects in space-time. While we know its effects on the matter side of EFE, the action on the gravitational part, i.e. the Ricci scalar, is defined in accordance with [53] as

$$\mathcal{R}(x) = \int dy \mathcal{A}^2(\square)\delta(x-y)R(x). \quad (5.3)$$

Let me repeat once more: While the field equations (5.1) represents spacetime coupled to a quasi-classical source term  $\mathcal{T}_{\mu\nu}$  according to General Relativity, the field equations (5.2) describe equations for nonlocal spacetime coupled to a classical source term  $\delta(r)$  after modified rules of General Relativity.

In this chapter, I want to derive a nonlocal operator  $\mathcal{A}^{-2}(x)$  for the given smearing models  $H(r)$ . For  $L_* \rightarrow 0$ , this operator will vanish  $\mathcal{A}^{-2} \rightarrow 1$ .

The operator is linked to the notion used in this thesis with a Fourier transformation. Working in momentum space allows us to easily compute the inverse. The smeared energy-momentum tensor reads

$$\mathcal{T}_0^0 = M\mathcal{A}^{-2}(\square)\delta^{3+n}(\vec{x}). \quad (5.4)$$

It produces the matter density as introduced in section 2.5.2:

$$\mathcal{T}_0^0 = \frac{M}{\Omega_{n+2} r^{n+2}} \frac{dH(r)}{dr}. \quad (5.5)$$

Matching equations (5.4) and (5.5) means

$$\mathcal{A}^{-2}(\square)\delta(\vec{x}) = \frac{1}{\Omega_{n+2} r^{n+2}} \frac{dH(x)}{dx} \quad (5.6a)$$

Writing the dirac delta by its plane wave momentum space representation  $\delta(\vec{x}) = \int d^{3+n}p e^{+ipx}$  on the left hand side and inserting a  $1 = \mathcal{F}^{-1}\mathcal{F}$  by means of a double fourier transformation on the right hand side allows computing a solution for the operator in momentum space by means of a fourier transformation of the right hand side:

$$\Leftrightarrow \int dp^{3+n} \mathcal{A}^{-2}(\square) e^{ipx} = \frac{1}{\Omega_{n+2}r^{n+2}} \frac{dH(x)}{dx} \quad (5.6b)$$

$$\Leftrightarrow \int d^{3+n}p \mathcal{A}^{-2}(p^2) e^{ipx} = \int d^{3+n}p \underbrace{\left( \frac{1}{(2\pi)^{2+n}} \int d^{3+n}z \frac{1}{\Omega_{n+2}\|z\|^{n+2}} \frac{dH(\|z\|)}{d\|z\|} e^{-ipz} \right)}_{T_0^0(p)} e^{ipx} \quad (5.6c)$$

$$\Leftrightarrow \mathcal{A}^{-2}(p^2) = \frac{1}{(2\pi)^{2+n}\Omega_{n+2}} \int d^{3+n}z \frac{1}{z^{n+2}} \frac{dH(z)}{dz} e^{-ipz} \quad (5.6d)$$

Note that, by concept, the operator  $\mathcal{A}^{-2}$  is dimensionless. We therefore can switch the coordinate system  $(r, p) \rightarrow (z, q)$  without new prefactors.

## 5.1 Higher-dimensional Fourier Transformation

To solve (5.6d), one can integrate out all extra dimensional angles and effectively reduce the higher-dimensional fourier transformation of the radial symmetric function to a one dimensional one. Calling  $V(r) := \frac{H'(r)}{r^{n+2}}$  the higher dimensional Fourier kernel, an effective one-dimensional Fourier transformation is derived in this section. This is motivated by the well-known three dimensional procedure which is easier to read and given in appendix 5.2.2.

Start with the  $N = n + 3$ -dimensional fourier transformation and rewrite it into conventional polar coordinates:

$$\hat{V}(p) = \frac{1}{(2\pi)^{3+n}} \int d^{3+n}r e^{-i\vec{r} \cdot \vec{p}} V(r) \quad (5.7a)$$

$$= \frac{1}{(2\pi)^{3+n}} \int_0^\infty dr r^{2+n} \int_0^{2\pi} d\varphi \prod_{i=1}^{n+1} \int_0^\pi d\theta_i \sin^i(\theta_i) e^{-i\vec{r} \cdot \vec{p}} V(r) \quad (5.7b)$$

Now use the angle  $\theta_1$  for identification with the inner scalar product angle  $\vec{r} \cdot \vec{p} := rp \cos \theta_0$ . Substitute  $\int_0^\pi d\theta_1 \sin(\theta_1) = - \int_{-1}^{+1} d\cos \theta := \int_{-1}^1 dx$ . Integrating out *all other*  $n$  angles  $\theta_i$  as well as the angle  $\varphi$  gives a  $\Omega_{2+n}/2$  contribution, as the  $n + 3$ -sphere volume is given by  $\int d^{3+n}r = \int dr \Omega_{n+2} r^{n+2}$ . Divide it by the missing factor  $\int_0^\pi d\theta \sin(\theta) = 2$ , used for the scalar product substitution. One ends up with

$$= \frac{1}{(2\pi)^{3+n}} \frac{\Omega_{n+2}}{2} \int_{-1}^{+1} dx \int_0^\infty dr r^{2+n} V(r) e^{-irpx} \quad (5.7c)$$

$$= \frac{1}{(2\pi)^{3+n}} \frac{\Omega_{n+2}}{2} \int_0^\infty dr r^{2+n} V(r) \left[ \frac{1}{-ipr} e^{-iprx} \right]_{-1}^{+1} \quad (5.7d)$$

$$= \frac{1}{(2\pi)^{3+n}} \frac{\Omega_{n+2}}{2} \frac{i}{p} \left( \int_0^\infty dr r^{1+n} V(r) e^{-ipr} - \int_0^\infty dr r^{1+n} V(r) e^{+ipr} \right) \quad (5.7e)$$

In favour to write this line as an effective one dimensional Fourier transformation, transform the second integral in line (5.7e), first by switching the integral borders,  $\int_0^\infty dr = -\int_\infty^0 dr$ , second by variable substitution  $r := -r'$ . This inserts an alternating minus, depending on  $n$ , as  $r^{1+n}dr = (-1)^{1+n}(r')^{1+n}(-1)dr' = (-1)^n r' dr'$ . Note the substitution also toggles the sign of the integral borders, allowing to combine both integrals to

$$= \frac{1}{(2\pi)^{3+n}} \frac{\Omega_{n+2}}{2} \frac{i}{p} \int_{-\infty}^\infty dr r^{1+n} [V(r)\Theta(r) + (-1)^n V(-r)\Theta(-r)] e^{-ipr} \quad (5.7f)$$

$$= \frac{1}{2\pi} \int_{-\infty}^\infty dr v(r) e^{-ipr}. \quad (5.7g)$$

One derives an effective one dimensional Fourier transformation of the effective function

$$v(r) := \frac{1}{(2\pi)^{2+n}} \frac{\Omega_{2+n}}{2} \frac{i}{p} r^{1+n} [V(r)\Theta(r) + (-1)^n V(-r)\Theta(-r)]. \quad (5.8)$$

Note that the Heaviside step function  $\Theta(z)$ , which was used to combine the integrals from line (5.7e) to one in (5.7f) is understood on the complex plane as

$$\Theta(z) = \Theta(\operatorname{Re} z). \quad (5.9)$$

The requirement (5.9) must be only exactly fulfilled at the evaluation points of the integral, that is, the poles of  $v(r)$ . Therefore,  $\Theta(z)$  may be weaker defined. See appendix 5.2.2 for more details.

Issues may arise with holomorphy when Cauchy theorem is applied. This is discussed further in the appendix, realizing that solving the integral on the complex plane works in three dimensions, so it shall work in any higher number of dimensions. Note that this approach was also successfully applied to a GUP-inspired nonlocal operator in an ongoing work [44].

## 5.2 Deriving the bilocal smearing operator

We now can solve the  $\mathcal{A}^{-2}$  integral (5.6d) by rewriting it to an one-dimensional one. Inserting

$$V(r) = \frac{1}{\Omega_{n+2} r^{n+2}} \frac{dH(r)}{dr} \quad (5.10)$$

into equation (5.7f) results in the compact expression, valid for any dimension  $n$ :

$$\mathcal{A}^{-2}(p^2) = \frac{1}{(2\pi)^{3+n}} \frac{i}{2p} \int_{-\infty}^\infty dr \frac{H'(|r|)}{r} e^{-ipr}. \quad (5.11)$$

This equation can be solved with the residue theorem. Since in (5.11),  $r \equiv \|\vec{r}\| \geq 0$  and  $p \equiv \|\vec{p}\| \geq 0$ , there is only one integration contour for Jordan's lemma. For the forward Fourier transformation  $\mathcal{F}_1$ , as seen in (5.11), the contour is determined by requiring (for some constant  $\# > 0$  representing the momentum)

$$\lim_{r \rightarrow \pm i\infty} e^{-ipr} = 0 \Rightarrow e^{-i(+\#)(\pm i\infty)} = e^{\pm i\infty\#} = 0 \Rightarrow r \rightarrow -i\infty, \quad (5.12)$$

i.e. it is closed on the lower half complex plane ( $\operatorname{Im} r < 0$ ). For the inverse Fourier transformation  $\mathcal{F}_1^{-1}$ , it is closed on the upper half complex plane ( $p \rightarrow i\infty \Leftrightarrow \operatorname{Im} p > 0$ ).

### 5.2.1 Holographic modified Einstein equations

In the holographic model, insert  $h(r)$  to derive from (5.11) the expression (note there is no need for powers of  $L$  when switching to dimensionless coordinates)

$$\mathcal{A}^{-2}(q^2) = \underbrace{\frac{2+n}{(2\pi)^{3+n}} \frac{i}{2q}}_{f_0} \int_{-\infty}^\infty dz \left[ \underbrace{\frac{z^n}{(1+z^{2+n})^2}}_{f_+} \Theta(z) + \underbrace{\frac{(-1)(-z)^n}{(1+(-z)^{2+n})^2}}_{f_-} \Theta(-z) \right] e^{-iqz}. \quad (5.13)$$

The poles of  $f_+$  are the same as for  $f_-$ , just mirrored at the imaginary axis  $\text{Re}(z) = 0$ , in symbols  $f_+(z) = -f_-(-z)$ . The poles of  $f_+$  are given by

$$(1 + z^{2+n})^2 = 0 \Leftrightarrow z = (-1)^{\frac{1}{2+n}} = \exp\left\{\frac{i\pi + 2\pi ik}{n+2}\right\} \quad \forall k \in \mathbb{N}_0. \quad (5.14)$$

There are  $n+1$  unique poles, each to be counted twice due to the power of 2 in the denominator of  $f_+$ . Due to the integration contour (5.12), only the  $\frac{n+1}{2}$  unique poles in the region  $\text{Im}(z_0) \leq 0$  are taken into account. For  $f_+$ , only the  $\frac{n+1}{4}$  poles in the region  $\text{Re}(z_0) \geq 0$  are visible. Identify these poles by their set of angles in the complex phase,

$$\Phi_n = \{\varphi = \arg(z) : 1 + z^{n+2} = 0 \wedge \text{Im}(z) \leq 0 \wedge \text{Re}(z) \geq 0\} \quad (5.15)$$

$$= \left\{ \varphi = \pi \frac{1-2k}{n+2} : k \in \mathbb{N}_0 \wedge k \leq \frac{n}{4} \right\}, \quad (5.16)$$

and write  $e^{i\Phi_n} = \{z = e^{i\varphi} : \varphi \in \Phi_n\}$  to denote the set of complex numbers associated with  $\Phi_n$ . Note the number of angles  $|\Phi_n| = \lfloor \frac{n+1}{4} \rfloor$  is a step function, so it is unlikely that a more compact expression than the subsequent one can be derived for general  $n$ .

All poles  $z_0 \in e^{i\Phi_n}$  are of 2nd order, the residues are therefore given by

$$\text{Res}_{z \rightarrow z_0} f_+(z) e^{iqz} = \lim_{z \rightarrow z_0} \frac{d}{dz} (z - z_0)^2 f_+(z) e^{iqz} = \frac{\text{sign}(z_0) \bar{z}_0}{(n+2)} e^{iz_0 q} (1 - iz_0 q) \quad (5.17)$$

and enter the holographic  $\mathcal{A}^{-2}$  integral from (5.13) in a way that

$$\begin{aligned} \int dz (f_+(z)\Theta(z) + f_-(z)\Theta(-z)) e^{iqz} &= (2\pi i)(-1) \cdot \\ &\cdot \left( 2 \sum_{z_0 \in e^{i\Phi_n}} \text{Res}_{z \rightarrow z_0} f_+(z) + 2 \sum_{z_0 \in e^{i\Phi_n}} \text{Res}_{z \rightarrow z_0} f_-(z) \right). \end{aligned} \quad (5.18)$$

Note that due to symmetry of the poles, there are either poles  $z_0$  (produced by  $f_+$ ) and  $-z_0$  (produced by  $f_-$ ) which residues sum to the expression

$$\text{Res}_{z_0} f_+ e^{izq} + \text{Res}_{-z_0} f_- e^{izq} = \text{Res}_{z_0} f_+ e^{izq} - \text{Res}_{z_0} f_+ e^{-izq} = \frac{2i\bar{z}_0}{(2+n)^2} \sin(z_0 q), \quad (5.19)$$

or the  $f_+$  and  $f_-$  share a common pole at  $z_0 = -i$ , then

$$\text{Res}_{-i} f_+ e^{izq} = \frac{i}{n+2} e^{+q} (1 - q). \quad (5.20)$$

Note that poles at  $z_0 = -i$  only occur at integer  $n/4$ , that is  $n = 0, 4, 8, \dots$ . In favour to give a closed form result, one therefore cannot always apply the simplification rules (5.19) and (5.20). The overall result is given by

$$\mathcal{A}^{-2} = \frac{(2\pi)^{2+n}}{q} \sum_{\varphi \in \Phi_n} \text{sign}(z_0) \bar{z}_0 e^{iz_0 q} (1 - iz_0 q) \quad (5.21)$$

with  $z_0 = e^{i\varphi}$ . Without extra dimensions ( $n = 0$ ) is the only case where a purely real result can be given, for  $n > 0$  complex phases always survive in (5.21). For  $n = 0$  we get (with  $q = pL$ ):

$$\mathcal{A}^{-2} = \frac{1}{4\pi} \left( \frac{e^{-q}}{q} + e^{-q} \right). \quad (5.22)$$

Reinserting  $L$  and sending  $L \rightarrow 0$  gives  $\mathcal{A}^{-2} \rightarrow 1/4\pi$ . (There is missing some  $4\pi$  here to ensure  $\mathcal{A}^{-2} \rightarrow 1$ ).

### 5.2.2 Self-encoding modified Einstein equations

For self-encoding model, insert  $h_\alpha(r)$  into the integral for  $\mathcal{A}^{-2}$  as given in (5.11). For convenience, switch to a new dimensionless notation,  $L' := L/2^{1/\alpha}$  and  $z = r/L'$ ,  $q = pL'$ . With that notation, all poles will have radius 1. The integral reads:

$$\mathcal{A}^{-2}(q^2) = \underbrace{\frac{3+n}{(2\pi)^{3+n}} \frac{i}{2q}}_{f_0} \int_{-\infty}^{\infty} dz \left[ \underbrace{\frac{z^{1+n}}{(1+z^\alpha)^{\frac{3+n}{\alpha}+1}}}_{f_+} \Theta(z) + \underbrace{\frac{(-1)(-z)^{1+n}}{(1+(-z)^\alpha)^{\frac{3+n}{\alpha}+1}}}_{f_-} \Theta(-z) \right] e^{-iqz}. \quad (5.23)$$

As with the holographic model, I chose  $f_+(z) = -f_-(-z)$  and will therefore discuss only  $f_+$ . Its poles are given by

$$(1+z^\alpha)^{\frac{3+n}{\alpha}+1} = 0 \quad \Leftrightarrow \quad z = (-1)^{1/\alpha} = \exp \left\{ \frac{i\pi + 2\pi ik}{\alpha} \right\} \quad \forall k \in \mathbb{N}_0. \quad (5.24)$$

For arbitrary choices of  $\alpha \in \mathbb{R}_{\geq 0}$ , as they were physically discussed in section ??, the poles multiplicity in (5.24) is not an integral number. For the poles determination, this is not a problem, but for calculating residues it is.

Equation for  $n$ th order singularities of a function  $g(z)$ :

$$\text{Res}_{z \rightarrow a} g(z) = \frac{1}{(n+1)!} \lim_{z \rightarrow a} \frac{\partial^{n-1}}{\partial z^{n-1}} ((z-a)^n g(z)) \quad (5.25)$$

Ways to solve that for  $n := \frac{3+n}{\alpha}$ : Fractional calculus...

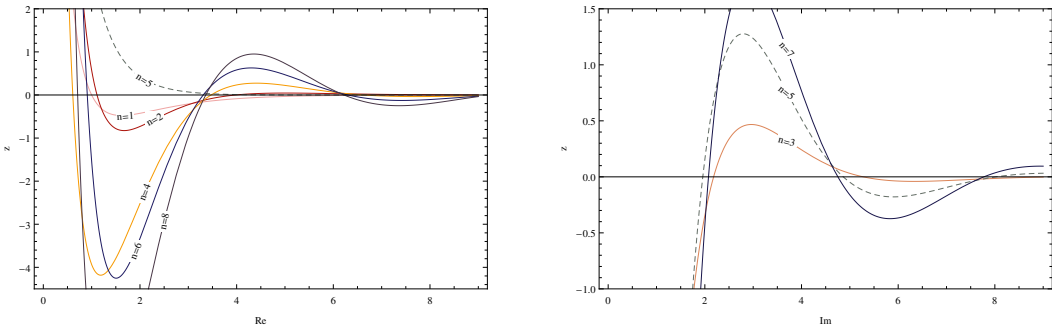


Figure 5.1: A placeholder picture for the upcoming plot of  $\mathcal{A}^{-2}(p)$ .

## 6 Conclusion

In this thesis, two self-encoding Black Hole geometries with their extra dimensional generalization are presented. The discussion was preceded by an introduction about the topics General Relativity, exact solutions, higher dimensional gravity scenarios and the quest for Quantum Gravity, namely by enumerating six Quantum Gravity theories that predict Black Holes.

Considering the geometry of the two self-encoding Black Holes, the concept of the Black Hole *remnant* is introduced and the parallel to the charged Reissner-Nordström Black Hole is showed. The de Sitter core as quantum vacuum source of outward pressure, stemming against the gravitational collapse, is introduced. For the self-encoding non-regular Black Hole, in this work referred to as the holographic Black Hole, the curvature singularity is hidden behind a horizon. This incorporates with the minimal length scenario, where distances smaller than the remnant size  $L_*$  and bigger than the reduced Planck mass  $M_*$  can not be probed. Physics in the trans-Planckian regime therefore gets unaccessible and shielded.

Regarding the thermodynamics of the self-encoding Black Holes, the remnants are found to be *cold* and *stable* in terms of a vanishing temperature and heat capacity. One finds logarithmic quantum corrections for the self-encoding holographic Black Hole in agreement with Loop Quantum Theory and String Theory. The holographic picture leads to area quantization and finally gives rise to an emergent gravity interpretation, explaining the gravitational force as entropic force.

As a last step, the *dual* theory to the self-encoding Black Holes is constructed. By means of finding the nonlocal operator that, applied on a Dirac delta distribution, produces just the desired distortion. This is a doorway of bringing the theory on a more fundamental level.

An appealing property of the geometries in this work is that one can do “paper and pen physics” without relying on numerical computations from the beginning. With the distinct feature of extra dimensions, this work pushes the underlying work forward on the “route to testable predictions” [56].

## Appendix

### A All forms of $H$

The choice  $H(r) = h(r)$  is called *holographic model* and the choice  $H(r) = h_\alpha(r)$  is called *self-encoding model* in this thesis. They are distinguished by the index  $\alpha$  on the  $h$ . Of course, one could also introduce a symbol like  $h_n(r)$  to account the fact that the models scale with  $n$ , so eventually the symbol is arbitrary.

In this appendix, we give the full forms in the dimensionless notation  $z = r/L$ . Since the models  $H(r)$  represent a smeared Theta function, they are dimensionless, and the identity  $h(r) = h(r/L)$  shall represent the fact that  $h(r)$  is actually a function of  $r/L$  and can be expressed in the dimensionless coordinate  $h(z)$ :

$$h(r) = \frac{r^{2+n}}{r^{2+n} + L^{2+n}} \quad h(z) = \frac{1}{1 + (\frac{1}{z})^{2+n}} = \frac{z^{2+n}}{z^{2+n} + 1} \quad (\text{A.26})$$

$$h_\alpha(r) = \frac{r^{3+n}}{(r^\alpha + L^\alpha/2)^{\frac{3+n}{\alpha}}} \quad h_\alpha(z) = \frac{1}{(1 + (\frac{1}{z})^\alpha / 2)^{\frac{3+n}{\alpha}}} \quad (\text{A.27})$$

The derivatives appear in many places and are therefore denoted here. Since  $\frac{df}{dr} = \frac{df}{dz} \frac{dz}{dr} = \frac{1}{L} \frac{df}{dz}$ , we can always substitute  $H'(r) = H'(z)/L$ . It is important to remember this fact:  $H'(r) \neq H'(z)$ . In the end, this is because the Lagrange differential operation notation  $H'$  is not unique.

$$h'(r) = \frac{(2+n)r^{1+n}L^{2+n}}{(r^{2+n} + L^{2+n})^2} \quad h'(z) = \frac{(2+n)(\frac{1}{z})^{3+n}}{\left(1 + (\frac{1}{z})^{2+n}\right)^2} = (2+n)\frac{h^2(z)}{z^{3+n}} \quad (\text{A.28})$$

$$h'_\alpha(r) = \frac{(3+n)L^\alpha r^{n+2} \left(\frac{L^\alpha}{2} + r^\alpha\right)^{-\frac{n+3}{\alpha}}}{L^\alpha + 2r^\alpha} \quad h'_\alpha(z) = \frac{\frac{3+n}{2}(\frac{1}{z})^{\alpha+1}}{\left(1 + (\frac{1}{z})^\alpha / 2\right)^{\frac{3+n}{\alpha}+1}} \quad (\text{A.29})$$

The dimensional analysis allows to resemble the powers of  $L$  in any expression written in terms of  $z$ . For example, the quantity  $H'(z)/z$  has the unit  $1/L^2$  and therefore  $H'(z)/(zL^2) = H'(r)/r$ .

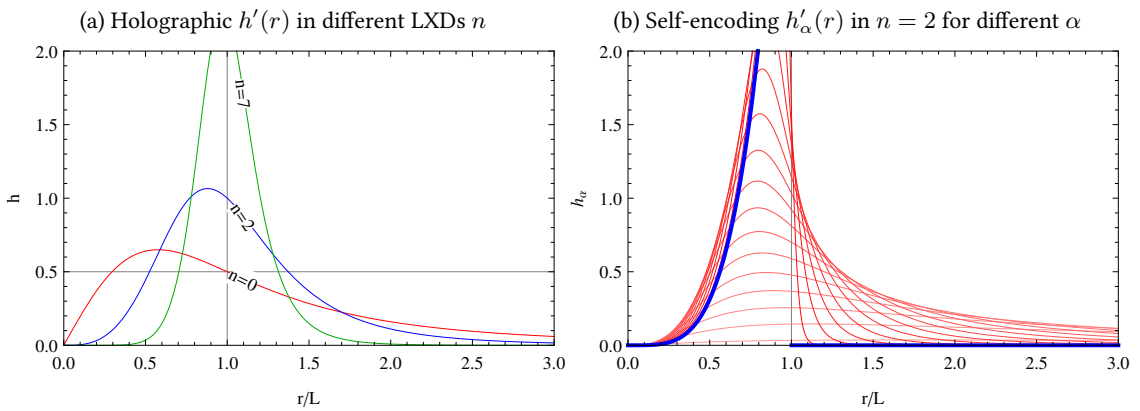


Figure A.2: The delta approximation functions in units of  $z = r/L$ . One clearly sees that a finite  $L > 0$  produces *nonlocality*. These plots just show the derivative of figure 2.3, as  $\frac{d\Theta}{dr} = \delta(r)$ .

## B $n$ -spheres

To point the emergence of  $n$ -spheres in this thesis, we evaluate the  $d$ -dimensional volume integral in euclidian space in spherical coordinates  $k_i = (r, \phi, \theta_1, \dots, \theta_{d-2})$ , following Wagner [74]:

$$\int d^d r = \int_0^\infty dr r^{d-1} \underbrace{\int_0^{2\pi} d\phi \prod_{j=1}^{d-2} \int_0^\pi d\theta_j \sin^j(\theta_j)}_{=a_{n-2}, \text{ since } (n-2)\text{-Surface}} = \frac{2\pi^{d/2}}{\Gamma(\frac{d}{2})} \int_0^r dr r^{d-1} := \Omega_{d-1} r^d := V_d \quad (\text{B.30})$$

where  $\Gamma(x)$  is the Euler Gamma function, given by

$$\Gamma(x) = \int_0^\infty dt t^{x-1} e^{-t} \quad ; \text{ incomplete version: } \gamma(s, x) = \int_0^x t^{s-1} e^t dt, \quad \Gamma(1/2) = \sqrt{\pi}, \quad (\text{B.31})$$

and the integration of the  $d - 2$  angles is done with the help of the identities

$$B(x, y) = \int_0^1 dt t^{x-1} (1-t)^{y-1} = \frac{\Gamma(x)\Gamma(y)}{\Gamma(x+y)} \quad (\text{B.32})$$

$$\int_0^\pi \theta_j \sin^j(\theta_j) = \frac{\sqrt{\pi} \Gamma(\frac{j+1}{2})}{\Gamma(\frac{j+2}{2})}. \quad (\text{B.33})$$

The  $n$ -sphere  $S_n$  with radius  $r$  is defined in an  $n$ -dimensional manifold (in this work always the euclidian space) by the set

$$S_n = \{ |\mathbf{x}| = r \mid \mathbf{x} \in \mathbb{R} \} \quad (\text{B.34})$$

In this work, the  $n$ -sphere is important for integration in spherical coordinates without angular dependence (isotropy or spherical symmetry). Integrating out the angles in a  $d$ -dimensional volume integration results in the surface area of the  $(d-1)$ -sphere, embedded in the  $d$ -dimensional space.

Formulas to remember for the volume of an  $n$ -ball and its corresponding  $(n-1)$ -sphere:

$$V_n = r^n \frac{\pi^{n/2}}{\Gamma(\frac{n}{2} + 1)} \quad \text{and} \quad A_{(n-1)} = \frac{dV_n}{dr} = \frac{\pi^{n/2}}{\Gamma(\frac{n}{2} + 1)} nr^{n-1} = 2 \frac{\pi^{n/2}}{\Gamma(\frac{n}{2})} r^{n-1} \quad (\text{B.35})$$

There also exists recursion relations for determining  $V_n, A_n$  by their lower dimensional values. For the sake of completeness, I also give definitions of the Gamma function  $\Gamma$ :

$$\begin{aligned} \Gamma(x) &= (x-1)! & \text{Prefactors:} & \quad V_n = v_n r^n & \text{Recursion:} & \quad v_0 = 1, \quad v_{n+1} = a_n/(n+1) \\ \Gamma(x+1) &= x\Gamma(x) & & \quad A_n = a_n r^n & & \quad a_0 = 2, \quad a_{n+1} = 2\pi v_n \end{aligned} \quad (\text{B.36})$$

I typically split the  $r$ -dependence in favour to dimensionless constants by  $A_n = \Omega_n r^n$  and  $V_n = \mathcal{V}_n r^n$ . For numerical values see table B.1.

$d$	0	1	2	3	4	5	6
$\mathcal{V}_d$	0	2	$\pi$	$\frac{4}{3}\pi$	$\frac{1}{2}\pi^2$	$\frac{8}{15}\pi^2$	$\frac{1}{6}\pi^3$
$\Omega_d$	0	2	$2\pi$	$4\pi$	$2\pi^2$	$\frac{8}{3}\pi^2$	$\pi^3$

Table B.1: Volume and surface area prefactors of  $d$ -Spheres.

## C Details of the radial symmetric $d$ -dimensional FT

This appendix ties up with section 5.1, where the  $d$ -dimensional Fourier Transformation is reduced to a one dimensional one for functions  $V(\vec{x})$  which fulfill  $V(\vec{x}) = V(|\vec{x}|)$ .

The 3d case is actually well known in literature and is given here just for completeness and simpler readability in section 5.2.2. In section 5.2.2, we discuss about entire function aspects of  $\Theta(z)$ .

### C.1 Review of the 3d Fourier transformation

We start the derivation in  $d = 3$  total spatial dimensions ( $\vec{r} \in \mathbb{R}^3$ ). Let  $V = V(r)$  with  $r = |\vec{r}|$  be a radially symmetric potential. Then its fourier transformation is given by:

$$\hat{V}(p) = \frac{1}{(2\pi)^3} \int d^3r e^{-i\vec{r}\cdot\vec{p}} V(r) \quad (\text{C.37a})$$

$$= \frac{1}{(2\pi)^3} \int_0^\infty dr \int_0^\pi r^2 \sin \theta d\theta \int_0^{2\pi} d\varphi V(r) e^{-ipr \cos \theta} \quad (\text{C.37b})$$

In line (C.37b) we already wrote the scalar product with an inner angle  $\theta_2$ . We now substitute the radial angle  $\theta$  (the  $\theta$  which is part of  $\vec{r} = (r, \theta, \varphi)$ ) integration with a  $\cos \theta$  integration. This can be done because  $\frac{d \cos \theta}{d\theta} = -\sin \theta$  and so  $\int_0^\pi \sin \theta d\theta = -\int_{-1}^1 d \cos \theta := \int_{-1}^1 dx$ . We now identify  $\cos \theta := x$  with  $\cos \theta_1$  because they share the same domain, actually  $\theta, \theta_1 \in \{0, \pi\}$  (this is a standard procedure, one can also argue with rotating the coordinate systems). Integrating out  $\int_0^{2\pi} d\varphi = 2\pi$  in mind, we continue with:

$$= \frac{2\pi}{(2\pi)^3} \int_{-1}^{+1} dx \int_0^\infty dr r^2 e^{-iprx} V(r) \quad (\text{C.37c})$$

$$= \frac{1}{(2\pi)^2} \int_0^\infty r^2 dr V(r) \left[ \frac{1}{-ipr} e^{-iprx} \right]_{-1}^{+1} \quad (\text{C.37d})$$

$$= \frac{1}{(2\pi)^2} \frac{i}{p} \int_0^\infty r dr V(r) \{ e^{-ipr} - e^{+ipr} \} \quad (\text{C.37e})$$

$$= \frac{1}{(2\pi)^2} \frac{i}{p} \left\{ \int_0^\infty r dr V(r) e^{-ipr} - \int_0^\infty r dr V(r) e^{+ipr} \right\} \quad (\text{C.37f})$$

In line (C.37f), we splitted the integral, and we now make two recastings: At first, switching the integral borders, which inserts one **minus**:  $\int_a^b = -\int_b^a$  in (C.37g). Second, another substitution of the integration parameter  $r := -r'$  and therefore  $dr = -dr'$ . The two minus signs kill each other in (C.37h), so  $r dr = r' dr'$ . After substitution, we will call  $r'$  again  $r$ , which is totally valid.

$$= \frac{1}{(2\pi)^2} \frac{i}{p} \left\{ \int_0^\infty r dr V(r) e^{-ipr} + \int_\infty^0 r dr V(r) e^{+ipr} \right\} \quad (\text{C.37g})$$

$$= \frac{1}{(2\pi)^2} \frac{i}{p} \left\{ \int_0^\infty r dr V(r) e^{-ipr} + \int_{-\infty}^0 r' dr' V(-r') e^{-ipr'} \right\} \quad (\text{C.37h})$$

$$= \frac{1}{(2\pi)^2} \frac{i}{p} \int_{-\infty}^\infty r dr e^{-ipr} \{ V(r) \Theta(r) + V(-r) \Theta(-r) \} \quad (\text{C.37i})$$

$$= \frac{1}{(2\pi)^2} \frac{i}{p} \int_{-\infty}^\infty dr \{ r V(|r|) \} e^{-ipr} \quad (\text{C.37j})$$

$$= \frac{1}{2\pi} \int_{-\infty}^\infty dr v(r) e^{-ipr} \quad (\text{C.37k})$$

We derived an effective one dimensional fourier transformation of the new function ("kernel")

$$v(r) := \frac{i}{2\pi} \frac{r}{p} V(|r|) \quad (\text{C.38})$$

For shortness, my usual definition of  $v(r)$  differs from the one given in (C.38) in terms of non-complex prefactors. For the discussion, equation (C.37i) is the best starting point, as it contains the Heaviside step functions  $\Theta(\pm r)$ .

The most important issue with this calculation is the question of holomorphy. In these lines,  $\Theta(z)$  must be understood as

$$\Theta(z) = \Theta(\operatorname{Re} z). \quad (\text{C.39})$$

This definition is intrinsically nonholomorphic. On the other hand, as soon as  $\Theta$  is implemented as a smeared distribution, like continuing the integral of a Dirac delta approximation like the Cauchy distribution, this might be cured. Anyway, there is no ordering relation  $\leq_{\mathbb{C}}$  in the complex numbers, so the theta is likely to behave differently on the complex plane. In three dimensions this approach is well known and works.

Whats about the real and complex parts of this fourier transformation? By construction,  $V(|r|)$  is an even function (definition:  $f(x) = f(-x)$  is even,  $-f(x) = f(-x)$  is odd). Therefore  $r V(|r|)$  is an odd function. By Eulers formula  $e^{i\varphi} = \cos \varphi + i \sin \varphi$ , one quickly finds that the Fourier Transform of an even function includes only (also even) cos terms and the complex part vanishes, while the FT of an odd function only contains sin terms and the real part vanishes. The integral in (C.37j) is therefore only complex,  $\int dr rV(|r|)e^{-ipr} \in \mathbb{C} \setminus \mathbb{R}$ . But the prefactor makes the final result in (C.37j) completely real again. This can help as a quick check wether the computed result of the integral is correct.

## C.2 Analytic continuation of the Heaviside step function

The step function  $\Theta : \mathbb{R} \rightarrow \mathbb{R}$ , as given in

$$\Theta(x) = \begin{cases} 0 & \text{when } x < 0 \\ 1 & \text{when } x \geq 0 \end{cases}, \quad (\text{2.27 revisited})$$

obviously cannot be simply extended on the complex plane. Anyway, in section 5.1, we already formulated *weaker constraints* instead of  $\Theta(z) = \Theta(\operatorname{Re} z)$ , namely

- Step function behaviour only on the poles which are laid on the unit ring  $|z| = 1$
- Approximate step function behaviour.
- Freedom of poles for  $\Theta(z)$ , so it does not contribute with poles to  $v(z)$ .

Freedom of poles means, we cannot have a rational function, so all theta approximations introduced in this thesis leave the stage. Such a theta approximation may be given by

$$\Theta_k(z) = \frac{1}{1 + \exp(-2kz)}, \quad \text{and } \Theta(x) = \lim_{k \rightarrow \infty} \Theta_k(x) \text{ for } x \in \mathbb{R} \quad (\text{C.40})$$

Inserting  $z = e^{i\phi}$  gives... okay this is not true.

## D Detailed Tensors in the spherical symmetry calculation and a formulary

In this section, I use greek lowercase letters ( $\alpha\beta\dots\mu\nu\dots$ ) for all indices which may in general be running in 4 or  $4+n$  dimensions. Einstein sum convention is used, but summation symbols are given when special emphasize on the summation is intended.

1. Christoffels for Tensor

$$\Gamma_{ij}^k = \frac{g^{kl}}{2} (\partial_i g_{jl} + \partial_j g_{il} - \partial_l g_{ij}) \quad (\text{D.41})$$

2. Christoffel symmetry:

$$\Gamma_{\beta\gamma}^\alpha = \Gamma_{\gamma\beta}^\alpha \quad (\text{D.42})$$

3. Covariant derivative for covariant vector  $t$ :

$$\nabla_a t^\nu = \partial_a t^\nu + \Gamma_{ac}^\nu t^c \quad (\text{D.43})$$

4. Covariant derivative for a  $(2, 0)$  tensor  $A$ :

$$\nabla_\lambda A^{\mu\nu} = \sum_\delta \partial_\lambda A^{\mu\nu} + \Gamma_{\delta\lambda}^\mu A^{\delta\mu} + \Gamma_{\delta\lambda}^\nu A^{\mu\delta} \quad (\text{D.44})$$

5. Covariant derivative for a  $(1, 1)$  tensor  $A$ :

$$\nabla_a T_c^b = \partial_a T_c^b + \Gamma_{ad}^b T_c^d - \Gamma_{ac}^d T_d^a \quad (\text{D.45})$$

6. Energy conservation equation with sums

$$\sum_\mu \nabla_\mu T^{\mu\nu} = \sum_{\mu,\rho} \partial_\mu T^{\mu\nu} + \Gamma_{\rho\mu}^\mu T^{\rho\mu} + \Gamma_{\rho\mu}^\nu T^{\mu\rho} \quad (\text{D.46})$$

7. Lowering and raising indices

$$g_{\beta\gamma} A^{\alpha\gamma} = A_\beta^\alpha \quad (\text{D.47})$$

8. Metric identity

$$g^{\alpha\beta} g_{\beta\gamma} = g_{\gamma\beta} g^{\beta\alpha} = \delta_\gamma^\alpha \quad (\text{D.48})$$

9. Riemann Tensor

$$R_{\sigma\mu\nu}^\delta = \partial_\mu \Gamma_{\nu\sigma}^\delta - \partial_\nu \Gamma_{\mu\sigma}^\delta + \Gamma_{\mu\gamma}^\delta \Gamma_{\nu\sigma}^\gamma - \Gamma_{\nu\gamma}^\delta \Gamma_{\mu\sigma}^\gamma \quad (\text{D.49})$$

10. Ricci tensor (sign is convention)

$$R_{\mu\nu} = \pm R_{\mu\gamma\nu}^\gamma \quad (\text{D.50})$$

11.  $(1, 1)$ -form of Ricci tensor

$$R_b^a = g^{ca} R_{cb} \quad (\text{D.51})$$

## D.1 Christoffel symbols

The Christoffel symbols for a general  $d$ -dimensional isotropic static metric, the parametrization  $g_{tt} = -(1 - A(r))$ ,  $g_{rr} = 1/(1 - A(r))$  and the alternative parametrization  $g_{tt} = -e^{\nu(r)}$ ,  $g_{rr} = e^{-\nu(r)}$ . The index naming convention follows section 3.  $f'$  indicates the derivation  $\partial_r f(r)$ .

$$\Gamma_{tr}^t = \Gamma_{rt}^t = \frac{1}{2} g^{tt} \partial_r g_{tt} = \frac{1}{2} \frac{A'}{A-1} = \frac{\nu'}{2} \quad (\text{D.52})$$

$$\Gamma_{tt}^r = \frac{1}{2} g^{rr} \partial_r g_{tt} = \frac{1}{2} (A-1) A' = \frac{1}{2} e^{2\nu} \nu' \quad (\text{D.53})$$

$$\Gamma_{rr}^r = \frac{1}{2} g^{rr} \partial_r g_{rr} = \frac{1}{2} \frac{A'}{1-A} = -\frac{1}{2} \nu' \quad (\text{D.54})$$

$$\Gamma_{ri}^i = \Gamma_{ir}^i = \frac{1}{2} g^{ii} \partial_r g_{ii} = \frac{1}{r} \quad (\text{D.55})$$

$$\Gamma_{\phi\phi}^i = \frac{1}{2} g^{\phi\phi} \partial_i g_{\phi\phi} = -\cos(\theta_i) \sin(\theta_i) \quad (\text{D.56})$$

$$\Gamma_{r\phi}^\phi = \Gamma_{\phi r}^\phi = \frac{1}{2} g^{\phi\phi} \partial_r g_{\phi\phi} = \frac{1}{r} \quad (\text{D.57})$$

$$\Gamma_{\phi i}^\phi = \Gamma_{i\phi}^\phi = \frac{1}{2} g^{\phi\phi} \partial_i g_{\phi\phi} = \frac{1}{\tan(\theta_i)} \quad (\text{D.58})$$

## List of figures and tables

This list helps to find and identify figures; they are labeled by their size and type (illustration or plots) and marked if they were not self-made.

### List of figures

3d	illustrative plot without axis of the deSitter self-regular Black Hole	1
1d	illustrative plot that resembles the 3d title page plot	2
0.1	Illustration <i>cube of physics</i> taken from [60]	5
1.1	Illustration for closed loops in Riemann geometry	8
1.2	Illustrations for large extra dimensional concepts, modified from [16, 33, 43]	14
1.2a	Brane world physics	14
1.2b	Compactified extra dimensions	14
1.2c	Hoop conjecture	14
2.1	Illustration about the evaporation phases, taken and modified from [33]	17
2.2	Illustration about the Black hole and particle phases	18
2.2a	Schwarzschild Black Hole–particle duality	18
2.2b	Self complete gravity	18
2.3	Plots of the Heaviside approximation functions $H(r)$	23
2.3a	Holographic profile $h(r)$ in different LXD $s$ $n$	23
2.3b	Self-encoding profile $h_\alpha(r)$ in $n = 2$ for different $\alpha$	23
3.1	Large plots of the gravitational potential	26
3.1a	$g_{00}$ for the holographic metric ( $h$ )	26
3.1b	$g_{00}$ for the self-regular metric ( $h_\alpha$ ) with $\alpha = \alpha_0$	26
3.2	Big plot of the higher dimensional gravitation potentials	27
3.3	Plot of the curvature scalar	30
3.4	Metric plot of the self-regular limit $\alpha \rightarrow \infty$	30
3.5	Plot of the Reissner-Nördstrom and Bardeen potential	30
3.6	Penrose diagram of regular Black Holes, made on basis of [1] in a color fashion like [32]	32
4.1	Big temperature plots with extremal radii $r_C$	35
4.1a	Temperature of the holographic Black Hole, compared to the Schwarzschild BH	35
4.1b	Temperature of the self-encoding Black Hole, compared to the holographic BH	35
4.2	Big Heat capacity plots $C_T$ scaled around the extremal radius $r_C$	37
4.2a	Heat capacity of the holographic Black Hole, compared to the Schwarzschild BH	37
4.2b	Heat capacity of the self-encoding Black Hole, compared to the holographic BH	37
4.3	Three panel plot: Gravitational potential, temperature and heat capacity	39
4.4	Artistic illustration of the holographic principle, taken from [7]	40
5.1	A placeholder picture for the upcoming plot of $\mathcal{A}^{-2}(p)$	46
A.2	Plots of the Dirac delta approximation functions $H'(r)$	48
A.2a	Holographic $h'(r)$ in different LXD $s$ $n$	48
A.2b	Self-encoding $h'_\alpha(r)$ in $n = 2$ for different $\alpha$	48

### List of tables

3.1	Length and mass scales of the smeared Black Holes in higher dimensions	28
4.1	The laws of thermodynamics correspond with Black Hole thermodynamics	34
4.2	Critical radii and maximum temperatures	36
B.1	Volume and surface area prefactors of $d$ -Spheres	49

# Bibliography

- [1] Ansoldi, Stefano, “Spherical black holes with regular center: A Review of existing models including a recent realization with Gaussian sources”, *arXiv*, e-print, (2008). [[arXiv:0802.0330 \[gr-qc\]](#)]. (Cited on pages 27, 29, 31, 32, 33, and 53.)
- [2] Ashtekar, Abhay and Lewandowski, Jerzy, “Background independent quantum gravity: A Status report”, *Class.Quant.Grav.*, **21**, R53 (2004). [[DOI](#)], [[arXiv:gr-qc/0404018 \[gr-qc\]](#)]. (Cited on page 20.)
- [3] Aurilia, A. and spallucci, E., “Planck’s uncertainty principle and the saturation of Lorentz boosts by Planckian black holes”, *arXiv*, e-print, (2013). [[arXiv:1309.7186 \[gr-qc\]](#)]. (Not cited.)
- [4] Aurilia, Antonio and Spallucci, Euro, “Why the length of a quantum string cannot be Lorentz contracted”, *Adv.High Energy Phys.*, **2013**, 531696 (2013). [[DOI](#)], [[arXiv:1309.7741 \[hep-th\]](#)]. (Not cited.)
- [5] Barvinsky, A.O., “Nonlocal action for long distance modifications of gravity theory”, *Phys.Lett.*, **B572**, 109–116 (2003). [[DOI](#)], [[arXiv:hep-th/0304229 \[hep-th\]](#)]. (Cited on page 18.)
- [6] Barvinsky, A.O., “Aspects of Nonlocality in Quantum Field Theory, Quantum Gravity and Cosmology”, *arXiv*, e-print, (2014). [[arXiv:1408.6112 \[hep-th\]](#)]. (Cited on page 18.)
- [7] Bekenstein, Jacob D. and Kamajian, Alfred T., “Information in the Holographic Universe”, *Scientific American*, (December 17, 2005), p. ... (Cited on pages 40 and 53.)
- [8] Bleicher, Marcus and Nicolini, Piero, “Large Extra Dimensions and Small Black Holes at the LHC”, *J.Phys.Conf.Ser.*, **237**, 012008 (2010). [[DOI](#)], [[arXiv:1001.2211 \[hep-ph\]](#)]. (Cited on page 15.)
- [9] Bleicher, Marcus and Nicolini, Piero, “Mini-review on mini-black holes from the mini-Big Bang”, *Astron. Nachr.*, **335**, 605–611 (2014). [[DOI](#)], [[arXiv:1403.0944 \[hep-th\]](#)]. (Cited on pages 15 and 16.)
- [10] Bonanno, A. and Reuter, M., “Spacetime structure of an evaporating black hole in quantum gravity”, *Phys.Rev.*, **D73**, 083005 (2006). [[DOI](#)], [[arXiv:hep-th/0602159 \[hep-th\]](#)]. (Cited on page 20.)
- [11] Carr, B.J., “The Black Hole Uncertainty Principle Correspondence”, *arXiv*, e-print, (2014). [[arXiv:1402.1427 \[gr-qc\]](#)]. (Cited on page 19.)
- [12] Carr, Bernard, Modesto, Leonardo and Premont-Schwarz, Isabeau, “Generalized Uncertainty Principle and Self-dual Black Holes”, *arXiv*, e-print, (2011). [[arXiv:1107.0708 \[gr-qc\]](#)]. (Cited on page 19.)
- [13] Carroll, Sean M., *Spacetime and geometry: An introduction to general relativity*, (Addison Wesley, San Francisco, 2004). (Cited on pages 7 and 8.)
- [14] Casadio, R., “What is the Schwarzschild radius of a quantum mechanical particle?”, *arXiv*, e-print, (2013). [[arXiv:1310.5452 \[gr-qc\]](#)]. (Not cited.)
- [15] Casadio, Roberto, Micu, Octavian and Nicolini, Piero, “Minimum length effects in black hole physics”, *arXiv*, e-print, (2014). [[arXiv:1405.1692 \[hep-th\]](#)]. (Not cited.)

- [16] Cavaglia, Marco, “Black hole and brane production in TeV gravity: A Review”, *Int.J.Mod.Phys.*, **A18**, 1843–1882 (2003). [[DOI](#)], [[arXiv:hep-ph/0210296 \[hep-ph\]](#)]. (Cited on pages 14, 15, and 53.)
- [17] Dirkes, Alain R. P., Maziashvili, Michael and Silagadze, Zurab K., “Black hole remnants due to Planck-length deformed QFT”, *arXiv*, e-print, (2013). [[arXiv:1309.7427 \[gr-qc\]](#)]. (Not cited.)
- [18] Dvali, Gia and Gomez, Cesar, “Self-Completeness of Einstein Gravity”, *arXiv*, e-print, (2010). [[arXiv:1005.3497 \[hep-th\]](#)]. (Not cited.)
- [19] Dvali, Gia and Gomez, Cesar, “Self-Completeness of Einstein Gravity”, *arXiv*, e-print, (2010). [[arXiv:1005.3497 \[hep-th\]](#)]. (Not cited.)
- [20] Dvali, G. and Gomez, C., “Minimal length and black hole area quantization”, *Fortsch.Phys.*, **59**, 579–585 (2011). [[DOI](#)]. (Cited on page 41.)
- [21] Dvali, Gia and Gomez, Cesar, “Black Hole’s Quantum N-Portrait”, *Fortsch.Phys.*, **61**, 742–767 (2013). [[DOI](#)], [[arXiv:1112.3359 \[hep-th\]](#)]. (Cited on page 41.)
- [22] Dymnikova, Irina, “Cosmological term as a source of mass”, *Class.Quant.Grav.*, **19**, 725–740 (2002). [[DOI](#)], [[arXiv:gr-qc/0112052 \[gr-qc\]](#)]. (Cited on pages 27 and 29.)
- [23] Elizalde, Emilio and Hildebrandt, Sergi R., “The Family of regular interiors for nonrotating black holes with  $T_0(0)=T_1(1)$ ”, *Phys.Rev.*, **D65**, 124024 (2002). [[DOI](#)], [[arXiv:gr-qc/0202102 \[gr-qc\]](#)]. (Cited on page 29.)
- [24] Emparan, Roberto and Reall, Harvey S., “Black Holes in Higher Dimensions”, *Living Rev.Rel.*, **11**, 6 (2008). [[arXiv:0801.3471 \[hep-th\]](#)]. (Cited on page 12.)
- [25] Falls, Kevin, Litim, Daniel F. and Raghuraman, Aarti, “Black Holes and Asymptotically Safe Gravity”, *Int.J.Mod.Phys.*, **A27**, 1250019 (2012). [[DOI](#)], [[arXiv:1002.0260 \[hep-th\]](#)]. (Cited on page 20.)
- [26] Fließbach, T., *Allgemeine Relativitätstheorie*, Spektrum Lehrbuch, 5. Auflage, (Spektrum-Akademischer Vlg, Heidelberg, 2006). (Cited on page 7.)
- [27] Frolov, V. and Novikov, I.D., *Black Hole Physics: Basic Concepts and New Developments*, Fundamental Theories of Physics, (Springer Netherlands, 1998). (Cited on page 17.)
- [28] Giddings, Steven B., “Possible observational windows for quantum effects from black holes”, *arXiv*, e-print, (2014). [[arXiv:1406.7001 \[hep-th\]](#)]. (Not cited.)
- [29] Gingrich, Douglas M., “Noncommutative geometry inspired black holes in higher dimensions at the LHC”, *JHEP*, **1005**, 022 (2010). [[DOI](#)], [[arXiv:1003.1798 \[hep-ph\]](#)]. (Not cited.)
- [30] Goenner, Hubert F. M., “On the History of Unified Field Theories”, *Living Reviews in Relativity*, **7**(2) (2004). [[DOI](#)]. URL (accessed September 2014): <http://www.livingreviews.org/lrr-2004-2>. (Cited on page 13.)
- [31] Griffiths, J.B. and Podolský, J., *Exact Space-Times in Einstein’s General Relativity*, Cambridge Monographs on Mathematical Physics, (Cambridge University Press, Cambridge, 2009). (Cited on pages 10, 11, 12, and 31.)
- [32] Hayward, Sean A., “Formation and evaporation of regular black holes”, *Phys.Rev.Lett.*, **96**, 031103 (2006). [[DOI](#)], [[arXiv:gr-qc/0506126 \[gr-qc\]](#)]. (Cited on pages 29, 32, and 53.)
- [33] Hossenfelder, Sabine, “What black holes can teach us”, *arXiv*, e-print, (2004). [[arXiv:hep-ph/0412265 \[hep-ph\]](#)]. (Cited on pages 14, 16, 17, and 53.)
- [34] Hossenfelder, Sabine, “Minimal Length Scale Scenarios for Quantum Gravity”, *Living Reviews in Relativity*, **16**(2) (2013). [[DOI](#)]. URL (accessed September 2014): <http://www.livingreviews.org/lrr-2013-2>. (Not cited.)

- [35] Isi, Maximiliano, Mureika, Jonas and Nicolini, Piero, “Self-Completeness and the Generalized Uncertainty Principle”, *JHEP*, **1311**, 139 (2013). [[DOI](#)], [[arXiv:1310.8153 \[hep-th\]](#)]. (Cited on page 19.)
- [36] Isi, Maximiliano, Mureika, Jonas and Nicolini, Piero, “Self-Completeness in Alternative Theories of Gravity”, *arXiv*, e-print, (2014). [[arXiv:1402.3342 \[hep-th\]](#)]. (Cited on page 19.)
- [37] Kanti, Panagiota, “Black holes in theories with large extra dimensions: A Review”, *Int.J.Mod.Phys.*, **A19**, 4899–4951 (2004). [[DOI](#)], [[arXiv:hep-ph/0402168 \[hep-ph\]](#)]. (Cited on pages 14 and 15.)
- [38] Kanti, Panagiota and Winstanley, Elizabeth, “Hawking Radiation from Higher-Dimensional Black Holes”, *arXiv*, e-print, (2014). [[arXiv:1402.3952 \[hep-th\]](#)]. (Cited on pages 13 and 15.)
- [39] Kempf, Achim, Mangano, Gianpiero and Mann, Robert B., “Hilbert space representation of the minimal length uncertainty relation”, *Phys.Rev.*, **D52**, 1108–1118 (1995). [[DOI](#)], [[arXiv:hep-th/9412167 \[hep-th\]](#)]. (Cited on page 19.)
- [40] Kiefer, Claus, “Quantum gravity: General introduction and recent developments”, *Annalen Phys.*, **15**, 129–148 (2005). [[DOI](#)], [[arXiv:gr-qc/0508120 \[gr-qc\]](#)]. (Cited on page 20.)
- [41] Kiefer, Claus, *Quantum gravity*, International series of monographs on physics, 136, (Oxford Univ. Press, Oxford [u.a.], 2007), 2. ed. edition. (Cited on page 20.)
- [42] Koch, Benjamin, *Black hole production and graviton emission in models with large extra dimensions*, Ph.D. thesis, (Goethe-Universität Frankfurt, Frankfurt, 2007). [[ADS](#)]. (Cited on page 7.)
- [43] Koch, Benjamin, Bleicher, Marcus and Hossenfelder, Sabine, “Black hole remnants at the LHC”, *JHEP*, **0510**, 053 (2005). [[DOI](#)], [[arXiv:hep-ph/0507138 \[hep-ph\]](#)]. (Cited on pages 14, 15, 16, and 53.)
- [44] Köppel, Sven, Iso, Maximiliano, Knipfer, Marco, Mureika, Jonas and Nicolini, Piero, “Self-Completeness and the Generalized Uncertainty Principle in Extra Dimensions”, in preparation, (2014). (Cited on pages 19 and 44.)
- [45] Maldacena, Juan Martin, “Black holes in string theory”, *arXiv*, e-print, (1996). [[arXiv:hep-th/9607235 \[hep-th\]](#)]. (Cited on page 20.)
- [46] Misner, Charles, Thorne, Kip and Wheeler, John, *Gravitation*, (W. H. Freeman, New York, 1973). (Cited on pages 7, 9, 11, 29, and 31.)
- [47] Modesto, Leonardo, “Loop quantum black hole”, *Class.Quant.Grav.*, **23**, 5587–5602 (2006). [[DOI](#)], [[arXiv:gr-qc/0509078 \[gr-qc\]](#)]. (Cited on page 20.)
- [48] Modesto, Leonardo, “Super-renormalizable Quantum Gravity”, *Phys.Rev.*, **D86**, 044005 (2012). [[DOI](#)], [[arXiv:1107.2403 \[hep-th\]](#)]. (Cited on page 18.)
- [49] Modesto, Leonardo, Moffat, John W. and Nicolini, Piero, “Black holes in an ultraviolet complete quantum gravity”, *Phys.Lett.*, **B695**, 397–400 (2011). [[DOI](#)], [[arXiv:1010.0680 \[gr-qc\]](#)]. (Cited on pages 18 and 32.)
- [50] Myers, Robert C., “Tall tales from de Sitter space”, in Gomberoff, A. and Marolf, D., eds., *Lectures on Quantum Gravity*, Series of the Centro De Estudios Científicos, p. 12345. Springer, (2006). (Cited on page 12.)
- [51] Nicolini, Piero, “Noncommutative Black Holes, The Final Appeal To Quantum Gravity: A Review”, *Int.J.Mod.Phys.*, **A24**, 1229–1308 (2009). [[DOI](#)], [[arXiv:0807.1939 \[hep-th\]](#)]. (Cited on page 19.)
- [52] Nicolini, Piero, “Entropic force, noncommutative gravity and un-gravity”, *Phys.Rev.*, **D82**, 044030 (2010). [[DOI](#)], [[arXiv:1005.2996 \[gr-qc\]](#)]. (Not cited.)
- [53] Nicolini, Piero, “Nonlocal and generalized uncertainty principle black holes”, *arXiv*, e-print, (2012). [[arXiv:1202.2102 \[hep-th\]](#)]. (Cited on page 42.)

- [54] Nicolini, Piero, Mureika, Jonas, Spallucci, Euro, Winstanley, Elizabeth and Bleicher, Marcus, “Production and evaporation of Planck scale black holes at the LHC”, *arXiv*, e-print, (2013). [[arXiv:1302.2640 \[hep-th\]](#)]. (Cited on page 15.)
- [55] Nicolini, Piero, Smailagic, Anais and Spallucci, Euro, “Noncommutative geometry inspired Schwarzschild black hole”, *Phys.Lett.*, **B632**, 547–551 (2006). [[DOI](#)], [[arXiv:gr-qc/0510112 \[gr-qc\]](#)]. (Cited on pages 19 and 21.)
- [56] Nicolini, Piero and Spallucci, Euro, “Holographic screens in ultraviolet self-complete quantum gravity”, *Adv.High Energy Phys.*, **2014**, 805684 (2014). [[DOI](#)], [[arXiv:1210.0015 \[hep-th\]](#)]. (Cited on pages 21, 23, 24, 27, 28, 41, and 47.)
- [57] Nicolini, Piero and Spallucci, Euro, “Holographic screens in ultraviolet self-complete quantum gravity”, *Adv.High Energy Phys.*, **2014**, 805684 (2014). [[DOI](#)], [[arXiv:1210.0015 \[hep-th\]](#)]. (Cited on page 25.)
- [58] Nicolini, Piero and Winstanley, Elizabeth, “Hawking emission from quantum gravity black holes”, *JHEP*, **1111**, 075 (2011). [[DOI](#)], [[arXiv:1108.4419 \[hep-ph\]](#)]. (Cited on page 18.)
- [59] Niedermaier, Max and Reuter, Martin, “The Asymptotic Safety Scenario in Quantum Gravity”, *Living Reviews in Relativity*, **9**(5) (2006). [[DOI](#)]. URL (accessed September 2014): <http://www.livingreviews.org/lrr-2006-5>. (Cited on page 20.)
- [60] Penrose, Roger, *The large, the small and the human mind*, (Cambridge Univ. Press, Cambridge, 1997). (Cited on pages 5 and 53.)
- [61] Perez, Alejandro, “The Spin-Foam Approach to Quantum Gravity”, *Living Reviews in Relativity*, **16**(3) (2013). [[DOI](#)]. URL (accessed September 2014): <http://www.livingreviews.org/lrr-2013-3>. (Cited on page 20.)
- [62] Reuter, M., “Nonperturbative evolution equation for quantum gravity”, *Phys.Rev.*, **D57**, 971–985 (1998). [[DOI](#)], [[arXiv:hep-th/9605030 \[hep-th\]](#)]. (Cited on page 20.)
- [63] Rizzo, Thomas G., “Noncommutative Inspired Black Holes in Extra Dimensions”, *JHEP*, **0609**, 021 (2006). [[DOI](#)], [[arXiv:hep-ph/0606051 \[hep-ph\]](#)]. (Cited on pages 19 and 21.)
- [64] Rovelli, Carlo, “Loop Quantum Gravity”, *Living Reviews in Relativity*, **11**(5), 12345 (2008). [[DOI](#)]. URL (accessed September 2014): <http://www.livingreviews.org/lrr-2008-5>. (Cited on page 19.)
- [65] Scardigli, Fabio and Casadio, Roberto, “Gravitational tests of the Generalized Uncertainty Principle”, *arXiv*, e-print, (2014). [[arXiv:1407.0113 \[hep-th\]](#)]. (Not cited.)
- [66] Spallucci, Euro and Smailagic, Anais, “Black holes production in self-complete quantum gravity”, *Phys.Lett.*, **B709**, 266–269 (2012). [[DOI](#)], [[arXiv:1202.1686 \[hep-th\]](#)]. (Not cited.)
- [67] Spallucci, Euro and Smailagic, Anais, “Semi-classical approach to quantum black holes”, *arXiv*, e-print, (2014). [[arXiv:1410.1706 \[gr-qc\]](#)]. (Not cited.)
- [68] Stephani, Hans, Kramer, Dietrich, MacCallum, Malcolm, Hoenselaers, Cornelius and Herlt, Eduard, *Exact Solutions of Einstein’s Field Equations*, Cambridge Monographs on Mathematical Physics, (Cambridge University Press, Cambridge, 2003). (Cited on page 10.)
- [69] Susskind, Leonard, “Trouble for remnants”, *arXiv*, e-print, (1995). [[arXiv:hep-th/9501106 \[hep-th\]](#)]. (Not cited.)
- [70] Susskind, Leonard, “Singularities, Firewalls, and Complementarity”, *arXiv*, e-print, (2012). [[arXiv:1208.3445 \[hep-th\]](#)]. (Not cited.)
- [71] Susskind, Leonard and Uglum, John, “Black hole entropy in canonical quantum gravity and superstring theory”, *Phys.Rev.*, **D50**, 2700–2711 (1994). [[DOI](#)], [[arXiv:hep-th/9401070 \[hep-th\]](#)]. (Not cited.)

- [72] Thiemann, Thomas, “Lectures on loop quantum gravity”, *Lect.Notes Phys.*, **631**, 41–135 (2003). [[DOI](#)], [[arXiv:gr-qc/0210094 \[gr-qc\]](#)]. (Cited on page 20.)
- [73] Thiemann, Thomas, “Loop Quantum Gravity: An Inside View”, *Lect.Notes Phys.*, **721**, 185–263 (2007). [[DOI](#)], [[arXiv:hep-th/0608210 \[hep-th\]](#)]. (Cited on page 20.)
- [74] Wagner, Marc, “Quantum Field Theory II”, lecture notes, (2013). (Cited on pages 19 and 49.)
- [75] Wald, Robert M., *General Relativity*, (The University of Chicago Press, Chicago and London, 1984). (Cited on pages 7, 11, and 31.)
- [76] Wald, Robert M., “Teaching general relativity”, *arXiv*, e-print, (2005). [[arXiv:gr-qc/0511073 \[gr-qc\]](#)]. (Cited on page 7.)
- [77] Witten, Edward, “Anti-de Sitter space, thermal phase transition, and confinement in gauge theories”, *Adv.Theor.Math.Phys.*, **2**, 505–532 (1998). [[arXiv:hep-th/9803131 \[hep-th\]](#)]. (Not cited.)

## Acknowledgement

First of all, I want to thank Piero Nicolini for his patience and availability in the past year. His knowledge in people and papers was a great help to navigate in the quantum gravity landscape.

I would also like to thank Marcus Bleicher for kind FIAS hospitality and group supervision.

## Erklärung

Ich versichere hiermit, die vorliegende Arbeit selbständig verfasst und keine anderen als die angegebenen Quellen und Hilfsmittel verwendet zu haben. Alle Stellen der Arbeit, die wörtlich oder sinngemäß aus Veröffentlichungen oder aus anderen fremden Texten entnommen wurden, sind von mir als solche kenntlich gemacht worden. Ferner erkläre ich, dass die Arbeit nicht – auch nicht auszugsweise – für eine andere Prüfung verwendet wurde.

Frankfurt am Main, im Oktober 2014

Sven Köppel